OXFORD
SOT | Society of Toxicology
academic.oup.com/toxsci

Toxicological Sciences, 2023, **193(1)**, 62–79
https://doi.org/10.1093/toxsci/kfad029
Advance Access Publication Date: March 13, 2023
Research article

Pulmonary and neurological health effects associated with exposure to representative composite manufacturing emissions and corresponding alterations in circulating metabolite profiles

Li Xia,[1] Yoorae Noh,[2] Andrew J. Whelton,[2] Brandon E. Boor,[2] Bruce Cooper,[3] Nathanael I. Lichti,[4] Jae Hong Park,[1] Jonathan H. Shannahan[1,*]

[1]School of Health Sciences, College of Health and Human Sciences, Purdue University, West Lafayette, Indiana, USA
[2]Lyles School of Civil Engineering, Purdue University, West Lafayette, Indiana, USA
[3]Bindley Bioscience Center Metabolomic Profiling Facility, Purdue University, West Lafayette, Indiana, USA
[4]Bindley Bioscience Center, Purdue University, West Lafayette, Indiana, USA

*To whom correspondence should be addressed. E-mail: jshannah@purdue.edu.

Abstract

Cured-in-place pipe (CIPP) technology is increasingly being utilized to repair aging and damaged pipes, however, there are concerns associated with the public health hazards of emissions. CIPP installation involves the manufacture of a new plastic composite pipe at the worksite and includes multiple variable components including resin material, curing methods, and operational conditions. We hypothesize styrene-based composite manufacturing emissions (CMEs) will induce greater pulmonary inflammatory responses and oxidative stress, as well as neurological toxicity compared with nonstyrene CMEs. Further, these CME-toxicological responses will be sex- and time-dependent. To test the hypothesis, representative CMEs were generated using a laboratory curing chamber and characterized using thermal desorption-gas chromatography-mass spectrometry and photoionization detector. Styrene was released during staying, isothermal curing, and cooling phases of the process and peaked during the cooling phase. Male and female C57BL6/J mice were utilized to examine alterations in pulmonary responses and neurotoxicity 1 day and 7 days following exposure to air (controls), nonstyrene-CMEs, or styrene-CMEs. Serum styrene metabolites were increased in mice exposed to styrene-CMEs. Metabolic and lipid profiling revealed alterations related to CIPP emissions that were resin-, time-, and sex-dependent. Exposure to styrene-CMEs resulted in an influx of lymphocytes in both sexes. Expression of inflammatory and oxidative stress markers, including *Tnfα, Vcam1, Ccl2, Cxcl2, Il6, Cxcl1, Tgfβ1, Tgmt2*, and *Hmox1*, displayed alterations following exposure to emissions. These changes in pulmonary and neurological markers of toxicity were dependent on resin type, sex, and time. Overall, this study demonstrates resin-specific differences in representative CMEs and alterations in toxicity endpoints, which can potentially inform safer utilization of composite manufacturing processes.

Keywords: composite; cured-in-place pipe; emissions; volatile organic chemicals; pulmonary; neurotoxicity; inflammation; oxidative stress; acute; recovery; sex

There is increasing concern about the impacts of plastic production on the environment and human health. Previous studies have examined the content of emissions and the adverse effects of these emissions released directly from the various manufacturing processes (CIEL *et al.*, 2019). Plastic manufacturing utilizes monomers to form polymers through polymerization reactions. Most monomers have limited biodegradability and are known toxicants (Hahladakis *et al.*, 2018). Monomers are often mixed with additives to improve performance such as flexibility, rheology, and elasticity (Hahladakis *et al.*, 2018). Base polymers such as polyvinyl chloride (PVC), polystyrene, and polyethylene have been demonstrated to cause adverse health effects including cardiovascular toxicity, endocrine disruption, reproductive or developmental damage, and pulmonary toxicity (Meeker *et al.*, 2009; Moore, 2008; Priyanka and Dey, 2018; Ramadan *et al.*, 2020; Thompson *et al.*, 2009). For instance, epidemiologic studies revealed inhaled heated PVC fumes were associated with asthma and respiratory symptoms in occupational settings (Jaakkola and Knight, 2008). Additionally, exposure to 3-D printer emissions from acrylonitrile butadiene styrene filament induced elevated levels of IFN-γ and IL-10 in the bronchoalveolar lavage (BAL) in exposed rats (Farcas, 2020). Plastic additives—phthalates, bisphenol A, and polybrominated diphenyl ethers can interact with multiple estrogen receptor subtypes interrupting transcriptional processes and/or signaling events in mammals (Priyanka and Dey, 2018). Moreover, exposure to bisphenol A in drinking water increased CD4+ T cells, IFN-γ, IL-17A, TLR4, caspase-1, and IL-1β in the heart resulting in myocardial inflammation, enhanced cardiac fibrosis, and elevated susceptibility of viral infection (Bruno *et al.*, 2019). Further, during the polymerization reaction, some organic chemicals such as methanol, cyclohexane, chloroform, dichloromethane, and benzoyl peroxide used as solvents and

initiators can be evaporated because of high temperature, vacuum, or continuous stirring. The evaporation of these chemicals and subsequent exposures may result in skin irritation and respiratory health issues (Hahladakis *et al.*, 2018; Lithner *et al.*, 2011).

In recent years, the cured-in-place pipe (CIPP) procedure, an outdoor plastic composite manufacturing process, has been utilized to repair buried water and sewer pipes. The CIPP procedure manufactures a new polymer composite within the damaged existing pipe, restoring its functionality. A flexible liner impregnated with resin is inflated in the damaged pipe and polymerized into a hard plastic. Polymerization of the resin into a new plastic liner inside the pipe is accomplished by exposing the resin to heat or ultraviolet light. Unsaturated polyester resins, vinyl ester resins, and epoxy resins are commonly used as raw materials, and styrene-based resins are the most popular and least expensive (Stratview Research, 2022).

With the growing use of the CIPP process to address aging infrastructure, concerns have been raised regarding the health hazards associated with emissions released into both the water and air during the composite manufacturing process (CDPH, 2017, 2020; FDOH, 2020; Lebouf, 2019; Noh *et al.*, 2022a; Ra *et al.*, 2019; Teimouri Sendesi *et al.*, 2017). The release of emissions has been associated with fish kills, water contamination, and HAZMAT responses (Tabor *et al.*, 2014). Recently, incidents near installation sites where CIPP-related emissions were released into the air were associated with evacuations of nearby schools and communities because of complaints of strong odors, dizziness, headaches, eye and respiratory irritation, shortness of breath, and nausea (Lebouf, 2019; Noh *et al.*, 2022b,c). Additionally, epoxy chemicals utilized in pipe relining were associated with a higher risk to develop allergic contact dermatitis among relining workers because of dermal exposure (Aalto-Korte *et al.*, 2015; Berglind *et al.*, 2012; Fillenham *et al.*, 2012). A variety of volatile organic compounds (VOCs) have been identified from CIPP installation worksites (Ajdari, 2016; Ra *et al.*, 2019; Teimouri Sendesi *et al.*, 2017). Also, a recent study using a laboratory curing chamber revealed 8 other VOCs in addition to styrene, including acetophenone, benzaldehyde, styrene oxide, cumene, α-methylstyrene, 1,2,3-trimethylbenzene (TMB), 1,3,5-TMB, and phenol in emissions generated from composite materials representative of those used in the CIPP manufacturing process (Noh *et al.*, 2023). Additionally, a previous study revealed discharge of nanoplastics from CIPP manufacture, whereas their influence on air quality and toxicity are still unclear (Morales *et al.*, 2022).

A few studies have examined outdoor and indoor environments near CIPP worksites and measured styrene, a primary component of many CIPP resins (Nuruddin *et al.*, 2019; Ra *et al.*, 2019; Teimouri Sendesi *et al.*, 2017, 2020). Styrene is classified as a Group 2B carcinogen, possibly carcinogenic to humans (IARC, 2002; NIEHS, 2021). The NIOSH exposure limit for styrene is 50 parts per million volume (ppm_v), and the United States Environmental Protection Agency (EPA) sets the acute exposure guideline level-1 at 20 ppm_v (IARC, 2002; NIEHS, 2021). Further, the California EPA Office of Environmental Health Hazard Assessment for CIPP installation identified 4.9 ppm_v as the acute reference exposure level for styrene exposure for the general public (CDPH, 2020). Previous studies reported styrene concentrations near a manhole exit at a CIPP worksite to be 1070 and 1824 ppm next to the resin tube delivery truck (Ajdari, 2016; Lebouf, 2019; Matthews, 2020; Ra *et al.*, 2019; Teimouri Sendesi *et al.*, 2017, 2020). The major acute health hazards associated with exposure to high levels of styrene include irritation of the respiratory tract and/or skin as well as central nervous system effects (Sumner and Fennell, 1994). Epidemiological assessments have demonstrated exposure to gas-phase styrene in occupational settings is associated with various nonmalignant pulmonary disorders, including bronchiolitis, hypersensitivity pneumonitis, and occupational asthma (Collins *et al.*, 2013; Kogevinas *et al.*, 1994; Meyer *et al.*, 2018). Additionally, styrene-exposed workers at plastic manufacturing facilities were determined to have diminished lung function and lung damage, as well as enhanced markers of oxidative stress and inflammation (Chakrabarti, 2000; Cherry and Gautrin, 1990; Kohn *et al.*, 1995; Sati *et al.*, 2011). Previously, an *in vitro* comparative toxicity assessment evaluated condensate samples collected from 3 CIPP worksites using styrene resins. This examination revealed differential cell death as well as alterations in expression of proteins involved in cell damage, immune responses, and cancer (Kobos *et al.*, 2019). Overall, this assessment of condensate samples suggested worksite and styrene-independent variations in CIPP-related emission toxicity.

There are numerous variations among worksites performing the CIPP procedure that may influence emissions and toxicity, including differences in resins, pipe conditions, environmental settings, and operations. Because styrene-based resins are associated with odor, nonstyrene-based CIPP resins are sometimes used as an alternative material. Therefore, our current study hypothesized styrene composite manufacturing emissions (CMEs) will induce greater pulmonary inflammatory responses and oxidative stress, as well as neurological toxicity compared with nonstyrene CMEs. Further, these CME-toxicological responses will be sex- and time-dependent. The specific objectives of this study are to characterize CMEs generated throughout the curing of styrene and nonstyrene-based resins, evaluate pulmonary and neurological toxicity endpoints, and determine distinct circulating biomarkers following exposure to CMEs. A laboratory curing system was used to generate and characterize representative CMEs to minimize complexities which may confound data interpretation because of multiple and variable CIPP worksite conditions in the laboratory (Noh *et al.*, 2023). This system was employed previously to produce representative styrene- and nonstyrene CMEs for characterization of chemical components (Noh *et al.*, 2023). To evaluate toxicity, male and female C57BL6/J mice were exposed once to freshly generated emissions or air (controls) and samples for analysis were collected 1- or 7-day postexposure.

Materials and methods

Animals

Male and female C57BL/6J mice (Jackson Labs, Bar Harbor, Maine) at 13 weeks of age were randomly assigned to 12 groups of 5. These groups represented 3 factors including sex (male and female), exposure (air [controls], styrene-CMEs, or nonstyrene-CMEs), and postexposure time points (1 day and 7 days). For each exposure group, 20 mice including 10 male mice and 10 female mice were randomly chosen after group housing. Five from each sex were placed in 4 different cells that were equally separated in the animal chamber. Sexes were alternated in each cell. After exposure, 5 mice from each sex were randomly selected for necropsy at 1-day postexposure for evaluation of acute responses, whereas the remaining 10 mice were necropsied 7-day postexposure to examine recovery following the single exposure. To eliminate potential variabilities caused by female sex hormones, the estrus cycle of female mice was synchronized through

transferring the bedding from the male mouse cage to the female mouse cage after group-housing for 1 week (Lundberg *et al.*, 2017; Yagielski, 2016). Mice in control and exposure groups were acclimated to chamber conditions 3 days prior to exposures. All mice were exposed at 15 weeks of age. A timeline diagram of the animal experimental details is depicted in Figure 1. All animal-related procedures were conducted under the National Institutes of Health guidelines and approved by the Purdue University Animal Care and Use Committee.

Exposure generation and system decontamination

Figure 2 is a schematic of the sampling chamber-environmental test chamber (ETC) setup used to generate CMEs (Noh *et al.*, 2023). It was previously utilized as a laboratory-based system to generate representative CMEs to characterize the volatile chemical emissions produced during the CIPP process (Noh *et al.*, 2023). Briefly, the composites were cured in the ETC and the emitted air was allowed to flow into the mouse exposure chamber. In this study, unsaturated polyester resin and vinyl hybrid resin were used as the styrene and nonstyrene resins, respectively. A resin mixture including resin base (styrene or nonstyrene) and initiators were impregnated into individual polyester felts (10.16 cm × 10.16 cm × 2.5 cm). Six layers of these felts were stacked vertically and cured in a heating oven. The curing process included 4 stages: (1) placing the felts in the oven for 1 h at ambient temperature (Staying), (2) heating the oven to 65.6°C for styrene resin impregnated felts and 82.2°C for nonstyrene resin impregnated felts (Preheating), (3) curing at a constant temperature for 50 min for styrene resin impregnated felts or 30 min for nonstyrene resin impregnated felts (Isothermal curing), and (4) turning off the heat and cooling down the oven and the newly formed composites for 1 h (Cooling). The curing step time periods for styrene and nonstyrene composite manufacturing reflected the procedures at the CIPP worksites and allowed different resin impregnated felts to fully cure into composites (Teimouri Sendesi *et al.*, 2020). The total time for animal exposure was 3 and 2 h 40 min during the curing of styrene-based composite or the nonstyrene-based composite, respectively. This includes the time associated with the "Preheating" period which takes approximately 10 min. The chambers and tubing were disassembled and cleaned with methylene chloride and acetone 3 times after every run followed by 10 min of pressurized air flushing. The disassembled components were then placed in an oven at 200°C for 48 h. After reassembling, the chamber was dried at ambient temperature for 24 h with ultra-zero grade air, consisting of 76.5%–80.5% nitrogen and 19.5%–23.5% oxygen (Airgas, Radnor, Pennsylvania) at the flow rate of 1.4 l/min. System decontamination was verified by measurement with sorbent tubes and photoionization detector (PID).

Exposure and exposure characterization

VOC concentrations were measured with ultra-zero grade air flowing through the system without composite materials inside the curing oven to verify no background residual contamination. These measurements were utilized as background to compare with VOC concentrations during the CME exposures. During the animal CME exposures, composites were cured to produce emissions via 4 stages: staying, preheating, isothermal curing, and cooling. Air samples during the mouse exposures were collected once in the middle of the staying, isothermal curing, and cooling stage by sorbent tubes. No sample was collected during preheating stage. A low-cost VOC sensor, PID, was also used for real-time monitoring of the styrene concentration according to the manufacturer's instructions. Before each experiment, the PID was calibrated using ultra-zero grade air and 10 ppm isobutylene. This calibrated PID response was then converted to styrene using the response factor 0.43 provided by the manufacturer. Air sampling was conducted at 30 min after placing composites in the chamber, 25 min or 15 min after beginning to cure styrene composite or nonstyrene composite, respectively, and 30 min after halting heating via PID and sorbent tube sample collection. The collected sorbent tube samples were analyzed by a Unity 2 Series thermal desorption (TD) system (Markes International, Inc, California) in conjunction with a gas chromatography (GC) (2010-Plus, Shimadzu, Inc, Maryland) and a mass spectrometry (MS) (TQ8040, Shimadzu, Inc, Maryland) to obtain the concentration of styrene. To insure there was no cross contamination, mice in the control group were exposed to filtered air only bypassing the curing oven with the same air sampling process.

Necropsy and sample collection

Mice were necropsied at 1- or 7-day postexposure. Blood, BAL fluid (BALF), lungs, brain, and liver were collected during the necropsy. Following euthanasia by injection of ketamine/xylazine (300 mg/kg; 90% ketamine/10% xylazine), blood was collected via cardiac puncture and serum isolated (centrifuging at 3500 × g at 4°C for 10 min). Serum was stored at −80°C for targeted and untargeted metabolite analysis (described below). BAL was then performed to collect BAL fluid from the right lung lobes. BAL is a minimally invasive procedure that involves instillation of sterile PBS buffer into the lung via trachea and is often utilized to evaluate acute lung injury following exposures (Gowdy, 2008; Hoecke, 2017; Komura, 2008; Russell, 2023; Tighe, 2018). Briefly, the left lung was tied off using a suture and 5 mm of a 1″ catheter was inserted into the trachea. The catheter was connected to a 1-ml syringe preloaded with a volume of PBS buffer determined based on the individual mouse's weight (17.5 ml/kg). Following instillation of the PBS into the right lung lobes, the fluid was allowed to

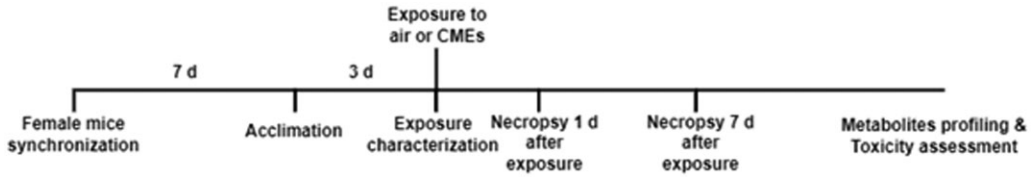

Figure 1. Timeline of animal study. After arrival, 13-week-old mice were randomly placed in cages. Female mice estrous cycles were synchronized and all mice were acclimated to exposure chamber 3 days prior to exposures. During exposures, photoionization detector (PID) and gas chromatography-mass spectrometry (GC-MS) were used to monitor and characterize CMEs. Half of the mice were necropsied 1 day after exposure to determine acute responses. The other half of the mice was necropsied at 7-day postexposure to examine recovery. Assessment of serum styrene-specific metabolites was performed to determine exposure whereas serum metabolite and lipid profiling were utilized to identify biomarkers of exposure and biological response. Assessment of toxicity endpoints included alterations in bronchoalveolar lavage fluid (BALF) markers of inflammation and lung injury (immune cell influx, total protein concentration, cytokine/chemokine levels), gene expression of inflammatory, oxidative stress, and injury markers in the unlavaged lung tissue, and gene expression of inflammation and oxidative stress markers in brain tissue.

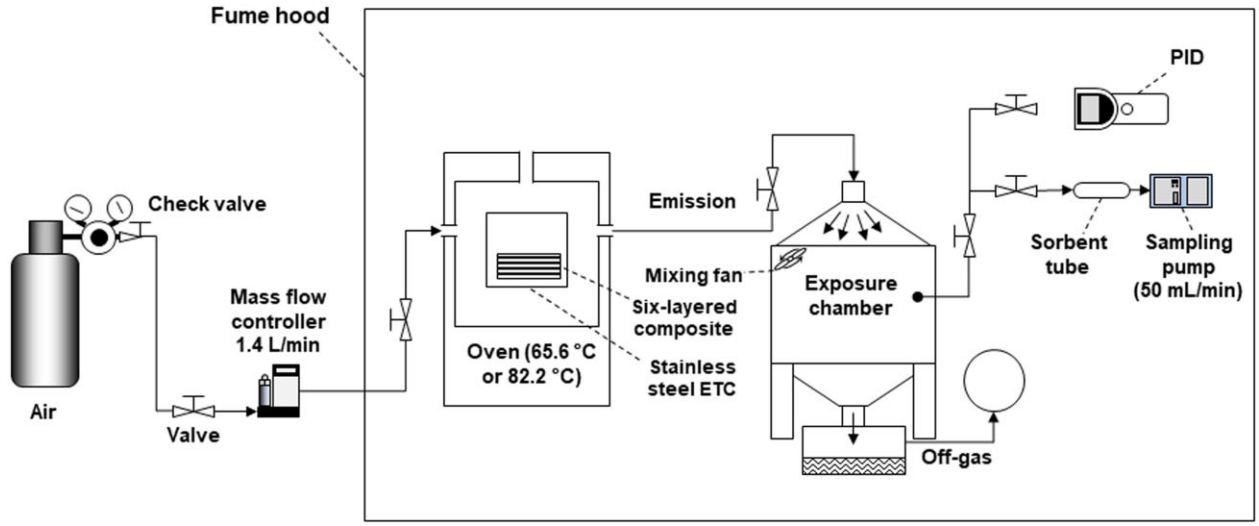

Figure 2. Sampling chamber-environmental test chamber (ETC) setup. Styrene and nonstyrene CMEs were produced within an oven and supplied to an exposure chamber housing 20 mice. PID measurements were made in real-time and air samples were collected using sorbent tubes for later characterization by GC-MS.

sit for 10 s prior to being collected. This lavage procedure was repeated for a total of 4 times using fresh volumes of PBS for each instillation. The first lavage volume was centrifuged at 1000 × g at 4°C for 10 min, and the supernatant fraction containing biomolecules was transferred to a 1.5-ml centrifuge tube and stored in a −80°C freezer for measurement of total protein concentrations and inflammatory cytokines/chemokines via enzyme-linked immunosorbent assay (ELISA). The cell pellet from the first lavage was combined with the cell pellet from all other 3 washes and resuspended in PBS for cell differentials. Left lung and brain were collected and stored at −80°C for real-time reverse transcription polymerase chain reaction (RT-PCR) assessments of alterations in gene expression of inflammatory and oxidative stress markers. Similar to other evaluations examining acute inhalation exposure-induced responses in pulmonary and brain tissues, mice were not perfused prior to organ collection (Gowdy, 2008; Komura, 2008; Smith, 2007).

Untargeted metabolite and lipid profiling

To examine if different CIPP-related emissions caused distinct global changes in metabolism, serum samples were processed via the Bligh and Dyer liquid-liquid extraction method and assessed by high-performance liquid chromatography with tandem mass spectrometry (HPLC-MS/MS). Briefly, 300 µl methanol was added to 100 µl serum samples and sonicated for 5 min. Then 300 µl chloroform and 200 µl water were added. The mixture was vortexed thoroughly followed by centrifugation for 5 min at 1000× *g*. This resulted in 2 phases, the upper polar phase (water/methanol) used the metabolite analysis, and the bottom organic phase (chloroform) was used for lipid analysis. After the phases were divided and dried in a vacuum concentrator, they were reconstituted for HPLC analysis. Seventy-five microlitres of 95% water, 5% acetonitrile, and 0.1% formic acid solution were added the for metabolites screening, whereas 75 µl of 30% acetonitrile, 50% methanol, and 20% water was added for lipid profiling. Five microlitres of samples were injected into an Agilent 1290 Infinity II UHPLC system coupled through electrospray ionization to a model 6445 quadrupole time-of-flight mass spectrometer (Q-TOF) (Agilent Technologies, Palo Alto, California). For metabolite analysis, a Waters Acquity HSS T3 (2.1 × 100 mm × 1.8 µm) separation column (Waters, Milford, Massachusetts) was used. Solvent A (0.1% formic acid in double-distilled water [ddH_2O]) and B (0.1% formic acid in acetonitrile) were the mobile phases. Flow rate was 0.45 ml/min. The gradient program utilized was 0–1 min, 0% B; 1–16 min, a linear gradient to 20% B; 16–21 min, a linear gradient to 95% B; the following 1.5 min, hold; and the last 1 min, returning to 0% B over 1 min. Then another 5 min were held to re-equilibrate the column. For mass spectrometric analysis, the Q-TOF was operated in MS-MS data dependent acquisition mode, acquiring mass spectral data from 70 to 1100 m/z in negative ionization mode.

For lipid analysis, a Waters BEH C18 (2.1 × 100 mm × 1.7 µm) separation column (Waters, Milford, Massachusetts) was used. Solvent A (10 mm ammonium acetate and 0.1% formic acid in ddH_2O) and B (10 mm ammonium acetate and 0.1% formic acid in 50% isopropyl alcohol:50% acetonitrile) were the mobile phases. Flow rate was 0.4 ml/min. The gradient program utilized was 0–0.5 min, 35% B; 0.5–5 min, a linear gradient to 20% B; 5–10 min, a linear gradient to 95% B; the following 5 min, hold; and the last 1 min, returning to 35% B over 1 min. Then another 5 min were held to re-equilibrate the column. For mass spectrometric analysis, the Q-TOF was operated in MS-MS data dependent acquisition mode, acquiring mass spectral data from 100 to 1200 m/z in positive ionization mode. The raw MS data were pre-processed in MS-DIAL (www.http://prime.psc.riken.jp), for deconvolution, alignment, and compound identification, and then statistically analyzed in R (R Core Team, 2015). Prior to analysis, the intensity data were filtered to remove features (metabolites or lipids) for which no experimental group (exposure * sex * time combination) had >2 nonzero intensity values, normalized to the sample medians, and log-2 transformed. Features in which all intensities were zero-valued in some experimental groups and not in others were classified as missing-not-at-random and randomly imputed on the log scale from a normal distribution centered at half the minimum intensity in the data, with a standard deviation equal to the mean standard deviation of the experimental groups. Values that were missing-at-random were not imputed.

Untargeted metabolite and lipid profiling—statistical analysis

After preprocessing, the intensities of each feature were analyzed using a univariate, 3-way ANOVA model based on exposures (control, styrene-CMEs, and nonstyrene-CMEs), sex (male and female), and time points (1 day and 7 days after exposure). Where necessary, robust linear models (Huber, 1981) were used to address unequal variance or outliers (Venables and Ripley, 1997). Pairwise comparisons among exposure levels were evaluated conditional on sex and time point using the emmeans package (Lenth *et al.*, 2022), and significant effects were tabulated after a global false discovery rate (FDR) correction to generate Venn diagrams. Metabolites or lipids with fold change >2 (ratio > 2 or <0.5; FDR < 0.05) were considered to differ significantly between groups. The number of common or unique candidates that were considered statistically different (FDR < 0.05) were compared through Venny 2.1.0 (https://bioinfogp.cnb.csic.es/tools/venny/) based on 3 factors including types of CMEs, postexposure time points, and sex. All candidates inside these criteria were listed after the removal of those only existing in nonmouse species.

Biomarkers of exposure—measurement of targeted styrene metabolites

After serum samples were isolated and extracted described above, the metabolite phase was utilized to measure styrene metabolites of interest, specifically styrene-7,8-oxide, mandelic acid, phenylglyoxylic acid, and phenylacetic acid, via liquid chromatography with tandem mass spectrometry (LC-MS/MS). An Agilent 1200 HPLC system was coupled to an Agilent 6460 series triple quadrupole mass spectrometer (Agilent Technologies, Santa Clara, California). A Waters T3 column (2.1 mm × 150 mm, 3 μm) was used for the separation. The buffers were: (A) water with 0.1% formic acid and (B) acetonitrile with 0.1% formic acid. The linear LC gradient was as follows: time 0, 5% B; 1 min, 5% B; 16 min, 20% B; 21 min, 95% B; 22.5 min, 95% B; 23.5 min, 5% B; 28.5 min, 5% B. The flow rate was 0.3 ml/min. Multiple reaction monitoring was used for MS analysis. Quantitation of each analyte was performed using a calibration curve. Detection limits for styrene-7,8-oxide, mandelic acid, phenylglyoxylic acid, and phenylacetic acid were 0.36, 0.89, 0.26, and 26.4 μg/ml, respectively.

Differential immune cell count and total protein concentration measurement in BALF

After BALF cell pellets were resuspended, total and differential cells were counted by a cellometer (Nexcelom, Massachusetts) to assess pulmonary alterations including an influx of immune cells in the cellular content of BALF. The same amount of BALF cells adhered to slides via 3 min centrifugation in a Cytospin IV (Shandon Scientific Ltd, Cheshire, United Kingdom) followed by being stained with a hematology statin (Thermo Fisher Scientific, Newington, New Hampshire). After the slides dried, they were observed and counted under bright-field microscopy. A total number of 300 cells were counted per slide from random fields on the slide. The number of differential immune cells in each BALF sample was then calculated based on the percentage of specific cell types in 300 cells and the total BALF cells.

The supernatant part of BALF containing rich proteins was used to evaluate the concentration of total proteins by Pierce BCA Protein Assay Kit (Thermo Fisher Scientific, Newington, New Hampshire). Briefly, 25 μl of standard solution or sample was added to a microplate well, then 200 μl of the working reagent (50:1, Reagent A:B) was added and mixed thoroughly with the standard or sample. The mixture was read in a microplate reader at 562 nm at room temperature.

mRNA expression analysis

Real-time RT-PCR was used to measure pulmonary and neurological inflammation and oxidative stress markers. Trizol (Invitrogen, Carlsbad, California) and ceramic beads (CK 14 soft tissue homogenizer Precellys, Bertin Technologies, Rockville, Maryland) were added to part of the left lung lobe samples for homogenization at a speed of 5 m/s for 1 min. Total RNA was extracted from the homogenate following isolation and purification by a Direct-zolTM RNA MiniPrep Kit (Zymo Research, Irvine, California) under the manufacturer's instructions. The concentration and quality of RNA samples were measured via a Nanodrop (Thermo Fisher Scientific, Newington, New Hampshire). An aliquot of 1 μg of RNA sample was reverse transcribed into Cdna through an iScriptTM Cdna Synthesis Kit (Bio-Rad, Hercules, California) under the manufacturer's instructions. Quantitative real-time RT-PCR analysis was performed to assess alterations of gene expression of inflammatory and oxidative stress markers including interleukin 6 (*Il6*), tumor necrosis factor-alpha (*Tnfα*), vascular cell adhesion molecule 1 (*Vcam1*), monocyte chemoattractant protein-1 (*Ccl2*), macrophage inflammatory protein-2 (*Cxcl2*), C-X-C Motif Chemokine Ligand 1 (*Cxcl1*), tumor growth factor-β1 (*Tgfβ1*), transglutaminase 2 (*Tgmt2*), and hemeoxygenase-1 (*Hmox1*) by utilizing predesigned primers (Integrated DNA Technologies, Inc, Coralville, Iowa). Gene expression of neurological inflammatory and oxidative stress biomarkers including *Il6*, *Tnfα*, *Vcam1*, *Cxcl2*, and *Hmox1* were assessed in the brain by real-time RT-PCR following the same protocol done in lung samples. Predesigned primers from Integrated DNA Technologies, Inc were used in this assessment. *Glyceraldehyde 3-phosphate dehydrogenase* (*Gapdh*) was used as the housekeeping gene for all genes. Relative fold gene expression of samples among different groups was calculated by using the delta-delta Ct method ($2^{-\Delta\Delta Ct}$) ($n = 5$/group). Additionally, 2 technical replicates for each sample were used in RT-PCR.

ELISA assays to evaluate BALF cytokine levels

Protein markers of inflammation in the supernatant from the first wash were evaluated. Commercially available mouse ELISA kits (R&D Systems, Inc, Minneapolis, Minnesota) were used to measure inflammatory cytokines in BALF, including IL6 and CXCL2 following the manufacturer's instructions. Briefly, 100 μl of diluted Capture Antibody was added to a 96-well microplate for an overnight plate coating. After that, the plate was rinsed 3 times with 400 μl of Wash Buffer each time. Then, the plate was blocked by adding 300 μl Reagent Diluent to each well for a minimum of 1 h followed by the same rinse 3 times done in earlier steps. When the plate was prepared, 100 μl of samples or standards, 100 μl of the Detection Antibody, and 100 μl of the working dilution of Streptavidin-HRP were added to per well in order and incubated for 2 h, 2 h, and 20 min, respectively, at room temperature. After incubation, 100 μl of Substrate Solution was added and incubated for 20 min at room temperature. This step should avoid direct light. Lastly, 50 μl of Stop Solution was added to each well. The data were read and collected at a wavelength of 540 nm in a microplate reader (Molecular Devices, San Jose, California). Two technical replicates for each sample were used in ELISA analysis.

Statistical analysis for targeted metabolites, cell differentials, gene expression, and BALF cytokines

Experiments for biological assessments were performed with an $n = 5$/group with 2 technical replicates. All data are presented as mean values ± SEM. Multi-comparison analysis of styrene metabolites, cell differentials, gene expression, and inflammatory responses were statistically assessed by 3-way ANOVA with Tukey *post hoc* analysis between groups, using exposure (styrene-CMEs or nonstyrene-CMEs), postexposure time point (1 day or 7 days), and sex (male or female) as the factors. Statistical significance was determined when p value $\leq .05$ between groups was determined. All statistical analyses were processed in GraphPad Prism 9 software (GraphPad, San Diego, California).

Results

Gas-phase styrene levels during mouse exposure

Twenty mice (10 males and 10 females) were placed into the exposure chamber and exposed to air (controls), styrene CMEs (styrene-CMEs), or nonstyrene CMEs (nonstyrene-CMEs). During these mouse exposures, emissions were sampled once in the middle of the staying, isothermal curing, and cooling phases. No VOCs were detected during background assessments when air was flowing through the system without material in the curing chamber. During the staying phase, styrene was not detected in the nonstyrene-CMEs (Table 1). Styrene was detected in the nonstyrene-CMEs during the isothermal curing and cooling phases (38.83 and 34.79 ppb, respectively) (Table 1). As expected, styrene was detected during all 3 phases assessed for the styrene-CMEs (Table 1). Styrene was 905.9 ppb during the staying stage, 569.6 ppb during the isothermal curing phase, and 3073 ppb during the cooling phase (Table 1). PID results demonstrated measurable emissions were produced during all phases for both resin materials (Table 1). The peak level of emissions was found during cooling down for both types of composites with styrene-based resins generating higher levels during each phase (Table 1). PID measurements were consistently higher than thermal desorption-gas chromatography-mass spectrometry (TD-GC-MS), ppm compared with ppb (Table 1).

Targeted styrene metabolite analysis

Serum was collected from mice at 1- and 7-day postexposure to identify styrene metabolites for exposure verification and to understand exposure kinetics. In the air group, no styrene-7,8-oxide or mandelic acid was detected at 1- or 7-day postexposure in both sexes (Table 2). A low level of phenylglyoxylic acid was observed in this group. Similar levels of these styrene metabolites were observed in the nonstyrene-CME group compared with the control group. Styrene-7,8-oxide, mandelic acid, and phenylglyoxylic acid were significantly increased in both male and female mice after 1-day exposure to styrene-CMEs (Table 2). There were no significant differences in styrene metabolites between male and female mice exposed to styrene-CMEs. A higher concentration of styrene-7,8-oxide was determined in serum than the levels of mandelic acid and phenylglyoxylic acid following exposure. At 7-day postexposure, styrene-7,8-oxide was still observed in the styrene-CMEs group, which was higher than its level at the 1-day time point (Table 2). More mandelic acid and phenylglyoxylic acid were detected in male mice, compared with the levels in controls and nonstyrene-CMEs groups, whereas their concentrations decreased compared with the 1-day time point.

Values are expressed as mean ± SEM ($n = 5$/group), the parentheses denote the number of mice from each group demonstrating levels above the detection limit for each metabolite. Phenylacetic acid was also measured but was not determined for all samples. Not determined (n.d.) denotes styrene-7,8-oxide < 0.36 μg/ml; mandelic acid < 0.89 μg/ml; phenylglyoxylic acid < 0.26 μg/ml; phenylacetic acid < 26.4 μg/ml. * denotes significant differences because of exposures compared with the control group matched for sex and time point, # denotes significant differences between styrene-CMEs and nonstyrene-CMEs matched for sex and time point, & denotes significant differences between male and female mice matched for exposure and time point, and $ denotes significant differences between 1- and 7-day postexposure time points matched for exposure and sex ($p < .05$).

Global metabolite profiling

There have been limited toxicological examinations of styrene- and nonstyrene-CMEs; therefore, to identify potential pathways and biomarkers of toxicity, serum samples were screened via metabolite profiling. Principal component analysis (PCA) of significantly altered metabolites determined differential grouping of male and female mice as well as alterations following emission exposures at 1- or 7-day postexposure time points (Supplementary Figure 1). Additionally, metabolite alterations determined to be statistically significant compared with controls ($p < .05$) were compared utilizing Venn diagrams (Figure 3). Specifically, these diagrams demonstrated unique and shared metabolites altered based on exposure (Figure 3A), time (Figure 3B), and sex (Figure 3C). Exposure to styrene-CMEs generated more unique metabolites compared with nonstyrene-CMEs (Figure 3A). At 7 days after exposure, fewer unique metabolites were identified in all mice exposed to styrene-CMEs compared with the number found at 1-day postexposure. The number of unique metabolites was observed to elevate in male mice exposed to nonstyrene-CMEs from 1 to 7 days, whereas there were no differences found in female mice (Figure 3B). Lastly, male and female mice also responded differently to the same exposure (Figure 3C). Different numbers of upregulated and downregulated metabolites were significantly altered in different

Table 1. Gas-phase styrene concentration in emissions from curing composites during mouse exposure

Nonstyrene-CMEs			Styrene-CMEs		
Phase of Manufacture	**TD-GC-MS (ppb)**	**PID (ppm)**	**Phase of Manufacture**	**TD-GC-MS (ppb)**	**PID (ppm)**
Mid-staying (30 min)	<Detection limit	35	Mid-staying (30 min)	905.9	245
Mid-isothermal curing (15 min)	38.8	45	Mid-isothermal curing (25 min)	569.6	310
Mid-cooling (30 min)	34.8	65	Mid-cooling (30 min)	3073	330

Time denotes at what point during the phase the samples were collected.

Table 2. Targeted styrene metabolites concentration in serum samples

Time Point	Comparison	Sex	Styrene Metabolite Serum Concentration (No. Mice Affected)		
			Styrene-7,8-Oxide (μg/ml)	Mandelic Acid (μg/ml)	Phenylglyoxylic Acid (μg/ml)
1 day	Control	Male	n.d.	n.d.	0.49 ± 0.04 (5)
		Female	n.d.	0.24 ± 0.21 (1)	0.75 ± 0.06 (5)
	Nonstyrene CMEs	Male	n.d.	n.d.	0.67 ± 0.03 (5)
		Female	n.d.	n.d.	0.66 ± 0.06 (5)
	Styrene CMEs	Male	29.68 ± 2.70 (5)*#	5.06 ± 0.92 (5)*#	7.06 ± 1.46 (5)*#
		Female	23.21 ± 2.49 (5)*#	5.67 ± 0.57 (5)#	5.91 ± 0.55 (5)#
7 days	Control	Male	11.18 ± 10.00 (1)	n.d.	0.31 ± 0.17 (2)
		Female	n.d.	n.d.	0.80 ± 0.07 (5)
	Nonstyrene CMEs	Male	n.d.	0.36 ± 0.32 (1)	0.27 ± 0.15 (2)$
		Female	n.d.	0.16 ± 0.14 (1)	0.41 ± 0.26 (2)
	Styrene CMEs	Male	44.75 ± 23.00 (4)	1.78 ± 0.96 (3)$	2.04 ± 0.63 (5)*#$
		Female	226.46 ± 169.22 (3)	15.54 ± 11.68 (3)	5.86 ± 3.97 (3)

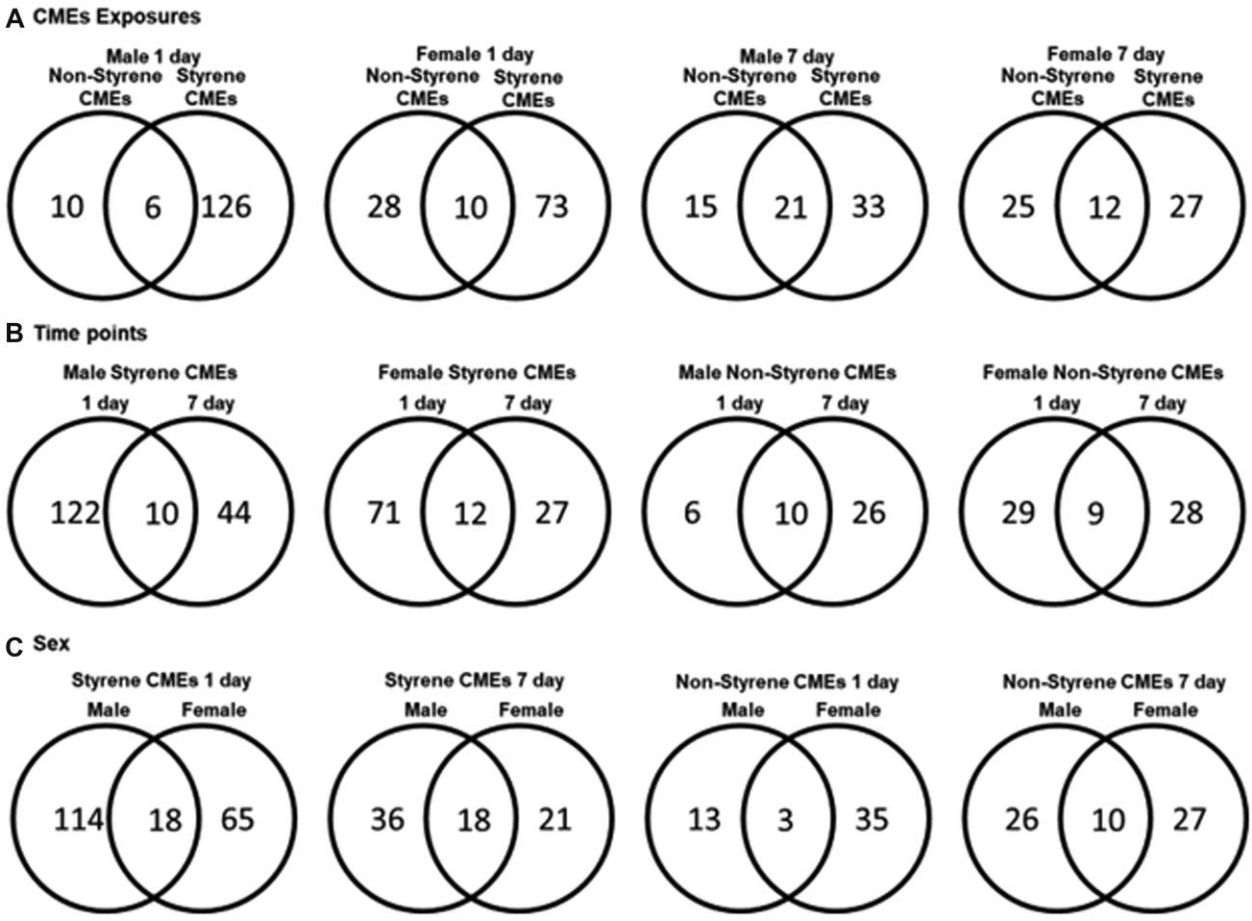

Figure 3. Venn diagrams of numbers of unique and shared metabolites with significance found in different comparisons based on (A) exposure (styrene-CMEs and nonstyrene-CMEs), (B) time point (1- and 7-day postexposure), and (C) sex (Male and Female) from untargeted metabolite profiling assessment of serum ($p < .05$). All metabolites used to generate Venn diagrams (A, B, C) can be found in Supplementary Table 1.

comparisons considering 3 factors: types of resin, postexposure time points, and sex (Table 3 and Supplementary Table 1). At 1-day postexposure, more metabolites demonstrated larger abundance in female mice in the styrene-CMEs exposure group compared with controls. However, fewer metabolites were upregulated in male mice of the same exposure and time group. Nonstyrene-CMEs demonstrated differences as more metabolites were determined to be upregulated in both sexes after exposure. At 7-day postexposure to styrene-CMEs, the total number of metabolites with significant changes decreased, but the opposite trend was observed in the nonstyrene-CMEs group compared with the controls. The relative abundance of metabolites of interest is listed in Table 4 and all significantly altered metabolites can be found in Supplementary Table 1.

Lipid profiling

Serum samples were also assessed through lipid profiling analysis to identify alterations of biomarkers and related pathways of

Table 3. Numbers of upregulated and downregulated serum metabolites found to be significantly different for comparisons of exposure (styrene-CMEs and nonstyrene-CMEs), sex (male and female), and time point (1- and 7-day postexposure)

			Metabolites Up/Downregulation	
Time Point	**Sex**	**Comparison**	**Upregulated**	**Downregulated**
1 day	Male	Styrene CMEs vs control	45	87
		Nonstyrene CMEs vs control	9	7
	Female	Styrene CMEs vs control	48	35
		Nonstyrene CMEs vs control	23	15
7 days	Male	Styrene CMEs vs control	27	27
		Nonstyrene CMEs vs control	15	21
	Female	Styrene CMEs vs control	21	18
		Nonstyrene CMEs vs control	24	13

emissions toxicity. PCA utilizing lipids determined to be significantly different from controls ($p < .05$) demonstrated differential grouping of mice following exposure to different emissions at 1- or 7-day postexposure time points (Supplementary Figure 2). Exposure to both CMEs showed different grouping from controls at both time points. There was no clear difference observed in terms of time point or sex. Venn diagrams suggested a number of unique and common lipids in comparisons considering 3 factors: exposures (Figure 4A), postexposure time points (Figure 4B), and sex (Figure 4C). Specifically, 1 day after exposure, male mice had more unique lipids identified in their serum following exposure to nonstyrene-CMEs compared with styrene-CMEs (Figure 4A). Numbers of unique lipids were found to increase in male mice exposed to styrene-CMEs and in females exposed to nonstyrene-CMEs at 7-day postexposure compared with the levels at 1-day time point (Figure 4B). Although less unique lipids were identified in male mice exposed to nonstyrene-CMEs and in females exposed to styrene-CMEs at 7-day postexposure compared with the levels at 1-day time point (Figure 4B). Male and female mice also responded very differently to similar exposures (Figure 4C). Additionally, abundances of lipids in serum were determined to be statistically significant based on exposure, sex, and time point. Among all significantly altered lipids ($p < .05$), the amount of upregulated and downregulated lipids are listed in Table 5. At the 1-day postexposure time point, more lipids were determined to be upregulated after exposure to both emissions in male and female mice, except for exposure to styrene-CMEs in female mice. Exposure to styrene-CMEs demonstrated differences in the abundance of lipids compared with the nonstyrene-CMEs. At 7 days after exposure, all exposures resulted in more upregulated lipids in both sexes. The relative abundance of lipids of interest is listed in Table 6 and all significantly altered lipids can be found in Supplementary Table 2.

BALF markers of pulmonary toxicity and inflammation

BALF total protein concentration, and differential immune cells were assessed 1 day or 7 days after exposure to CMEs to determine pulmonary injury and inflammation. The concentration of BALF total protein levels was elevated at 1 day after exposure to styrene-CMEs in both male and female mice (Figure 5A). After 7 days, no significant difference showed in total protein concentration following either CMEs exposure compared with the level in the air group (Figure 5A). Total cell counts, lymphocyte counts, and macrophage counts were altered because of emission exposures (Figs. 5B–D). Exposure to both CMEs resulted in a decreased number of total cells and macrophages after 1 day compared with controls (Figs. 5B and 5C). Elevated numbers of lymphocytes were observed 1-day postexposure to styrene-CMEs in both male and female mice (Figure 5D). At 7-day postexposure, slightly more lymphocytes were observed in mice exposed to styrene resin-CMEs.

Gene expression analysis of markers of inflammation in the lung

Inflammatory gene expression alterations were examined 1 day or 7 days following exposures. Significant increases in the inflammatory gene expression levels within lung tissue samples were observed because of exposures in both male and female mice including *Cxcl2*, *Il6*, *Ccl2*, *Tnfα*, *Vcam1*, *Cxcl1*, *Tgmt2*, *Hmox1*, and *Tgfβ1* (Figs. 6A–I). At 1-day postexposure, gene expression of *Cxcl2*, *Il6*, *Tgmt2*, *Hmox1*, and *Tgfβ1* were elevated in males exposed to styrene-CMEs whereas no significant increases were observed in males exposed to nonstyrene-CMEs. *Tnfα*, *Vcam1*, and *Cxcl1* were found to be elevated following exposure to emissions produced from manufacturing both composites in males. In females, *Il6* and *Ccl2*, and *Hmox1* were enhanced following styrene-CMEs exposure compared with the levels in control at 1-day postexposure. *Cxcl2*, *Tnfα*, *Vcam1*, *Hmox1*, and *Tgfβ1* were observed to be increased following exposure to nonstyrene-CMEs in female mice. *Hmox1* was the only gene determined to be elevated after both exposures in females at the 1-day time point (Figure 6H). At 7-day postexposure, *Cxcl2* and *Ccl2* were upregulated in male mice exposed to styrene-CMEs (Figs. 6A and 6C). These 2 genes did not show any differences in other exposure groups in both sexes compared with the levels in control at 7-day postexposure. Gene expression of *Cxcl1* increased in male mice exposed to both emissions at 7-day time point (Figure 6F). Other markers including *Il6*, *Tnfα*, *Vcam1*, *Hmox1*, and *Tgfβ1* did not show significant changes following either CMEs exposure in male and female mice at the 7-day postexposure time point (Figs. 6B, 6D, 6E, 6H, and 6I).

BALF inflammatory cytokines level

Protein expression of a representative cytokine and chemokine were examined within the BALF to determine alterations in pulmonary inflammation response to CIPP-related emissions. CXCL2 and IL6 were elevated in male and female mice 1 day after exposure to styrene-CMEs compared with the levels in control and nonstyrene-CMEs groups (Figure 7). No differences in the protein levels of CXCL2 and IL6 were observed at 7-day postexposure to either emission.

Gene expression analysis of markers of inflammation and oxidative stress in the brain

Gene expression of inflammatory markers was also examined to determine the potential for neurological effects following exposure. Gene expression of *Vcam1* was increased in male mice 1 day following exposure to emissions from both resins, whereas

Table 4. Representative serum metabolites determined to be significantly different because of exposure (styrene CMEs and nonstyrene CMEs), sex (male and female), and time point (1- and 7-day postexposure)

Time Point	Sex	Comparison	Representative Metabolites	Fold Change	*p* Value
1 day	Male	Styrene CMEs vs control	2-Amino-9-(6-aminopurin-9-yl)-1H-purin-6-one	5.28	.01
			Arctic acid B	3.83	.014
			6-[5-(carboxymethyl)-2-hydroxyphenoxy]-3,4,5-trihydroxyoxane-2-carboxylic acid	3.72	.041
			Dopamine 4-sulfate	3.68	.038
			10-Methyl-9-(10-methyl-1H-acridin-9-yl)-1 H-acridine	3.09	.004
			TG(18:3(6Z,9Z,12Z)/22:6(4Z,7Z,10Z,13Z,16Z,19Z)/O-18:0)	2.79	.034
		Nonstyrene CMEs vs control	2-Methoxyestrone 3-glucuronide	2.74	.0001
			Nirtetralin	2.56	.028
			1-(2,2-Difluoroethyl)pyrrolidine-3,4-dicarboxylic acid	2.26	.046
	Female	Styrene CMEs vs control	2-[4-hydroxy-3-(sulfooxy)phenyl]acetic acid	6.86	.029
			Homovanillin	5.44	.033
			Quinolacetic acid	4.89	.025
			TG(18:3(6Z,9Z,12Z)/22:6(4Z,7Z,10Z,13Z,16Z,19Z)/O-18:0)	4.31	.001
			N-(5-(5-(2,4-Dioxo-1,3,8-triazaspiro[4.5] decan-8-yl)pentanoyl)-2,4-dimethoxyphenyl)-4-(trifluoromethyl)benzenesulfonamide	3.83	.009
			5-Hydroxy-3-[[5-(4-nitrophenyl)furan-2-yl] methylideneamino]-1H-imidazol-2-one	2.34	.045
		Nonstyrene CMEs vs control	Oxydemeton-methyl	7.19	.021
			2-Amino-5-[[1-[carboxymethyl(sulfo) amino]-1-oxo-3-sulfanylpropan-2-yl] amino]-5-oxopentanoic acid	5.3	.003
			TG(18:3(6Z,9Z,12Z)/22:6(4Z,7Z,10Z,13Z,16Z,19Z)/O-18:0)	3.52	.015
7 days	Male	Styrene CMEs vs control	3,5-Dimethylphenol	6.18	.047
			Quinolacetic acid	5.72	.02
			2-[4-hydroxy-3-(sulfooxy)phenyl]acetic acid	5.3	.045
			3,5-Dihydroxyphenylvaleric acid sulfate	4.39	.003
			Imidazooxazole	4.07	.023
			5-Hydroxy-3-[[5-(4-nitrophenyl)furan-2-yl] methylideneamino]-1H-imidazol-2-one	1.52	.02
		Nonstyrene CMEs vs control	Imidazooxazole	4.86	.007
			LysoPG(18:2(9Z,12Z)/0:0)	3.02	.045
			6-[3-(carboxymethyl)phenoxy]-3,4,5-trihydroxyoxane-2-carboxylic acid	2.92	3.26×10^{-5}
			3,5-Dimethylphenol	2.75	.024
	Female	Styrene CMEs vs control	trans- and cis-2,4,8-Trimethyl-3,7-nona-dien-2-ol	4.12	.02
			N-Acetyl-DL-phenylalanine	2.94	.023
		Nonstyrene CMEs vs control	4-Aminoacetophenone	5.31	.009
			3,6-Dihydroxycyclohepta-2,4,6-trien-1-one	2.68	.035
			Dantrolene	2.53	5.49×10^{-5}
			2-Methoxyestrone 3-glucuronide	1.52	.025

female mice only demonstrated increases following exposure to styrene-CMEs compared with controls. *Tnfα* was enhanced following exposure to styrene-CMEs in males at 1-day postexposure. In females, *Tnfα* increased following both emission exposures at 1-day postexposure. At 7-day postexposure, gene expression levels of *Vcam1* remained elevated in both male and female mice in response to exposures (Figure 8A). Gene expression levels of *Tnfα* were enhanced following exposures to styrene-CMEs at 1-day postexposure in male and female mice (Figure 8B). After 7 days, female mice showed an increase in the gene expression of *Tnfα*, *Cxcl2*, *and Hmox1* only following exposure to styrene-CMEs (Figs. 8B, 8D, and 8E).

Discussion

Emissions resulting from the CIPP procedure have been associated with public health events (Noh *et al.*, 2023; Ra *et al.*, 2019; Teimouri Sendesi *et al.*, 2020). The present study investigated potential toxicity of representative CMEs by exposing male and female mice to emissions from the manufacture of styrene- and nonstyrene composites. Emissions were chemically characterized, and toxicity endpoints were examined. Styrene metabolite analysis confirmed exposure and supported resin differences in exposure. Exposure to CMEs resulted in elevated lung permeability, alterations in gene and protein expression of inflammatory and oxidative stress markers in lung and brain tissues, and unique serum metabolite and lipid profiles. Overall, results demonstrated differential alterations in pulmonary and neurological markers of toxicity which were dependent on resin type, sex, and time point.

The laboratory-based system used to generate CMEs enabled the creation of exposure conditions where potential toxicological consequences of emissions were evaluated (Noh *et al.*, 2023). Styrene-CMEs resulted in a peak styrene concentration of

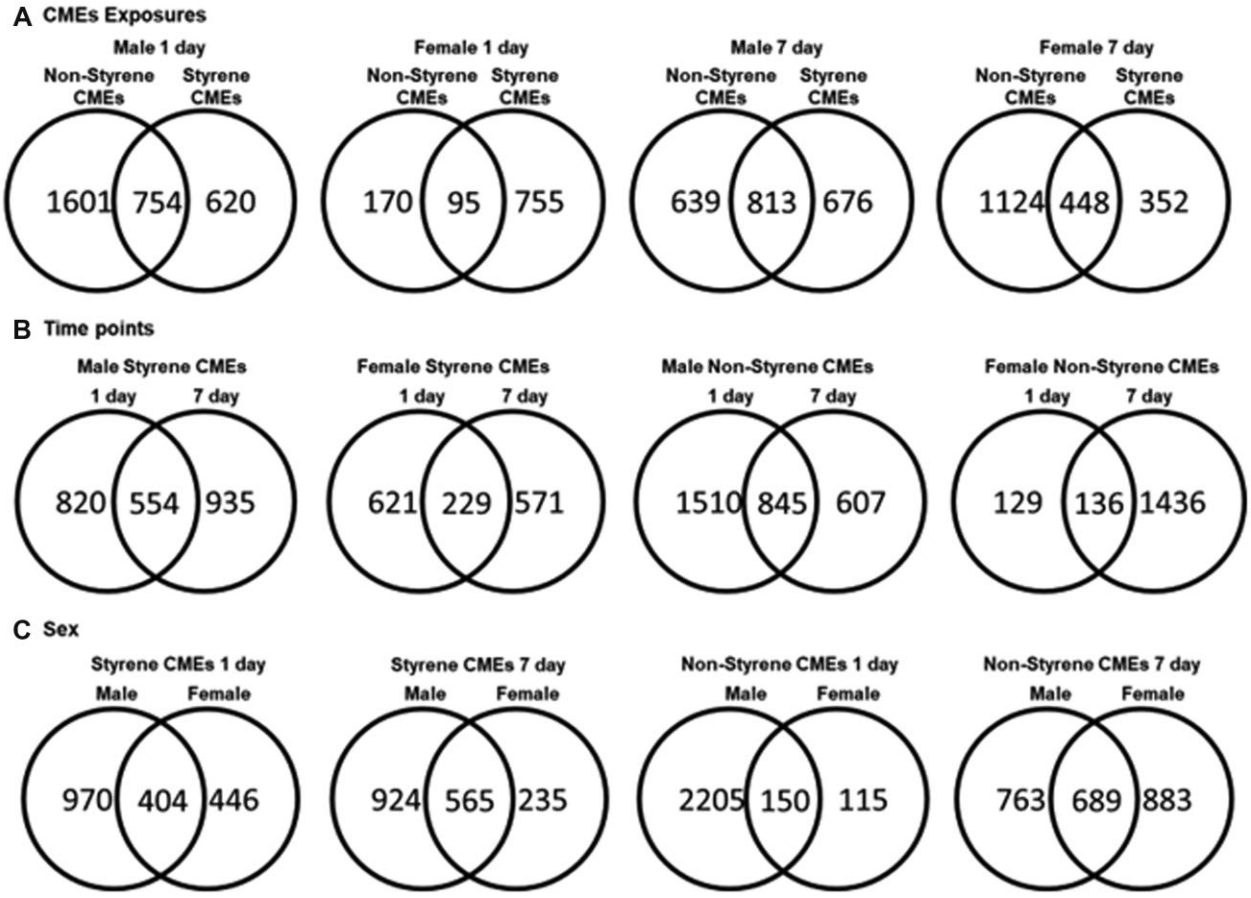

Figure 4. Venn diagrams of numbers of unique and shared lipids with significance found in different comparisons based on (A) exposures (styrene-CME and nonstyrene-CME), (B) time point (1- and 7-day postexposure), and (C) sex (male and female) from untargeted lipid profiling assessment of serum ($p < .05$). All lipids used to generate Venn diagrams (A, B, C) can be found in Supplementary Table 2.

3073 ppb during animal exposure (Table 1) which can be translated into a human exposure level of 15.4 ppm based on the surface area of the mouse respiratory system. This concentration is relevant based on previous styrene levels measured at CIPP instillation sites and regulations. Previous studies detected styrene under steam curing process near the sewer pipe manholes at 250–1070 ppm_v and 3.6–76.7 ppm_v during curing and cooling down, respectively (Ajdari, 2016; Teimouri Sendesi *et al.*, 2017), exceeding the immediately dangerous to life or health value for styrene of 700 ppm during the curing phase (NIOSH, 1994). The styrene threshold limit value set by the American Conference of Governmental and Industrial Hygienists (ACGIH) is 20 ppm averaged over an 8-h work shift which is comparable to our study's peak level (ACGIH, 2013). The California EPA Office identified 4.9 ppm as the acute reference exposure level for styrene exposure to the general public according to their Health Hazard Assessment for CIPP Installation (CDPH, 2020). The highest level of styrene in the styrene-CMEs appeared during the cooling stage and was still detectable at the end of the process in this study. This finding agreed with previous studies (Noh *et al.*, 2022b,c) indicating styrene continues to be released after active curing is halted. Here, both TD-GC-MS and PID methods were applied to examine styrene emissions; however, the PID overestimated styrene levels in the present study compared with those quantified via TD-GC-MS. This finding agrees with other studies that have demonstrated inconsistent quantification of styrene levels by calibrated PIDs for CIPP composites manufactured in the lab and in the field (Noh *et al.*, 2023; Ra *et al.*, 2019), possibly because of the PID responding to other VOCs besides styrene. Although often utilized to understand exposures, the PID may not be an accurate instrument to evaluate styrene within CIPP emissions.

Styrene is primarily absorbed into the bloodstream via inhalation in exposure settings. Several metabolites are formed during styrene metabolism, such as styrene oxide, styrene glycol, mandelic acid, phenylglyoxylic acid, hippuric acid, phenylethanol, vinylphenol, and hydroxyphenethyl. To understand the delivery of emissions to mice, specific metabolites including styrene-7,8-oxide, mandelic acid, and phenylglyoxylic acid were assessed in serum. These metabolites have been identified in mice following acute styrene inhalation to concentrations ranging from 125 to 500 ppm as well as in human CIPP workers (Morgan *et al.*, 1993b; Persoons *et al.*, 2018; Sumner and Fennell, 1994). Elevated urinary levels of styrene, mandelic acid, and phenylglyoxylic acid were determined among workers from 4 different plants or companies involved in plastic manufacturing, vehicle repair, and CIPP installation (Persoons *et al.*, 2018). Styrene-7,8-oxide is the primary metabolite in the styrene metabolism pathway, whereas mandelic and phenylglyoxylic acids are the secondary metabolites. Targeted mass spectrometry demonstrated significantly elevated levels of styrene-7,8-oxide, mandelic acid, and phenylglyoxylic acid 1 day following exposure to styrene-CMEs. Overall, the targeted metabolite assessment revealed the mice were exposed to CMEs. The nonstyrene-CMEs group showed limited changes in mandelic acid and phenylglyoxylic acid in serum, as expected.

Table 5. Numbers of upregulated and downregulated serum lipids found to be significantly different for comparisons of exposures (styrene-CME and nonstyrene-CME), sex (male and female), and time point (1- and 7-day postexposure)

			Lipids Up/Downregulation	
Time Point	**Sex**	**Comparison**	**Upregulated**	**Downregulated**
1 day	Male	Styrene CMEs vs control	778	596
		Nonstyrene CMEs vs control	1194	1161
	Female	Styrene CMEs vs control	395	455
		Nonstyrene CMEs vs control	140	125
7 days	Male	Styrene CMEs vs control	934	555
		Nonstyrene CMEs vs control	938	514
	Female	Styrene CMEs vs control	433	367
		Nonstyrene CMEs vs control	993	579

Table 6. Representative serum lipids determined to be significantly different because of exposures (styrene-CME and nonstyrene-CME), sex (male and female), and time point (1- and 7-day postexposure)

Time Point	**Sex**	**Comparison**	**Representative Lipids**	**Fold Change**	***p* Value**
1 day	Male	Styrene CMEs vs control	FAHFA 34:4; O	6.74	3.21×10^{-12}
			PA 24:0	6.67	1.69×10^{-8}
			PS O-37:0	4.71	4.94×10^{-12}
			PG 38:1	4.68	8.24×10^{-13}
		Nonstyrene CMEs vs control	PA 24:0	7.09	3.88×10^{-9}
			FAHFA 34:3; O	6.45	6.77×10^{-12}
			PA 26:4; O3	5.84	.003
			FA 23:1; O	5.65	.001
			PE 24:3; O2	5.09	.004
	Female	Styrene CMEs vs control	FAHFA 34:4; O	5.30	1.06×10^{-9}
			TG 49:8	4.95	2.29×10^{-11}
			PA 24:0	4.63	9.87×10^{-6}
			TG 48:1	4.59	8.57×10^{-13}
		Nonstyrene CMEs vs control	FAHFA 34:4; O	3.95	1.09×10^{-6}
			PA 24:0	3.82	.0002
7 days	Male	Styrene CMEs vs control	PA 24:0	6.84	8.97×10^{-9}
			FAHFA 34:4; O	5.94	5.67×10^{-11}
			PS 31:0	5.14	.004
			PS O-36:6	4.97	.003
		Nonstyrene CMEs vs control	PA 24:0	6.38	4.76×10^{-8}
			FAHFA 34:4; O	5.81	1.05×10^{-10}
			PI 32:0	4.84	.003
	Female	Styrene CMEs vs control	PA 44:8	11.32	5.46×10^{-12}
			PS 37:2	11.12	4.38×10^{-12}
			PG 38:3	10.87	5.26×10^{-12}
			PA 44:8	10.52	6.77×10^{-12}
			PS O-38:2	10.39	1.58×10^{-11}
			PA 44:7	9.85	5.24×10^{-12}
			FA 11:0; O2	9.62	8.24×10^{-13}
			PC 37:1	9.50	2.98×10^{-12}
		Nonstyrene CMEs vs control	PA 44:8	9.63	3.30×10^{-10}
			PS 37:2	9.30	3.63×10^{-10}
			PG 38:3	9.16	3.96×10^{-10}

No sex differences in metabolism of styrene were observed 1 day after exposures, which agrees with a previous study that did not find significant differences in levels of blood styrene oxide between males and females exposed to 125 or 250 ppm (Morgan *et al.*, 1993a). Circulating styrene metabolite levels were time point dependent as at 7-day postexposure, metabolites were reduced, likely because of the half-life of styrene ranging between 7 and 16 h (Rosemond, 2010).

Limited data exist regarding the toxicity of CMEs; therefore, metabolite and lipid screening approaches were utilized to identify potential biomarkers and toxicity pathways. Numerous metabolites and lipids were altered following exposure to CMEs that were resin material-, time point-, and sex-specific. Many of these were associated with inflammation, oxidative stress, and disease progression. For example, results demonstrated an elevated abundance of Triglyceride (18:3(6Z,9Z,12Z)/22:6(4Z,7Z,10Z,13Z,16Z,19Z)/O-18:0), FAHFA 34:4; O, and Phosphatidic acid 24:0 following exposure to both emissions at 1-day postexposure in both sexes. Triglyceride accumulation in serum is associated with inflammation and increased risk of heart disease (Patel, 2004; Welty, 2013), FAHFA 34:4; O is involved in regulating glucose metabolism and inflammation (Wood, 2020) and phosphatidic acid is associated with the secretion of proinflammatory cytokines (Lim *et al.*, 2003). These metabolites/lipids such as Triglyceride (18:3(6Z,9Z,12Z)/22:6(4Z,7Z,10Z,13Z,16Z,19Z)/O-18:0), FAHFA 34:4; O, and Phosphatidic acid 24:0 represent potential styrene- and sex-independent biomarkers of acute CME exposure. They could be potentially useful as general biomarkers for acute exposure to CMEs. However, variabilities exist at composite manufacturing worksites in terms of engineering parameters and weather conditions as well as individuals may demonstrate variable responses to exposure because of sex, metabolism, and susceptibility which may

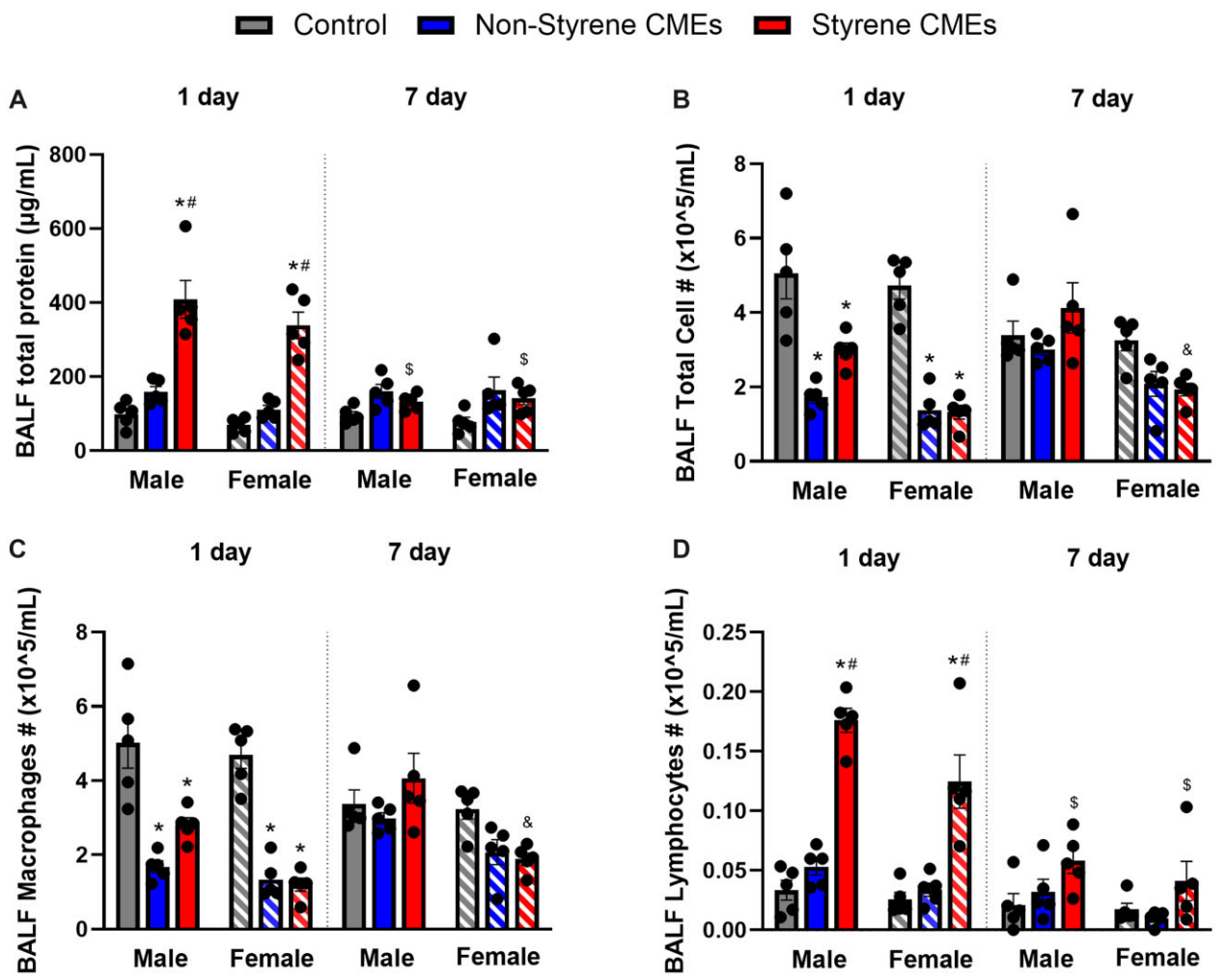

Figure 5. Bronchoalveolar lavage fluid (BALF) total protein concentration (A), total cell counts (B), macrophage counts (C), and lymphocyte counts (D) in BALF at 1 day or 7 days after exposure to nonstyrene-CMEs, or styrene-CMEs in male and female mice ($n = 5$/group). * denotes significant differences because of exposures compared with the control group matched for sex and time point, # denotes significant differences between styrene-CMEs and nonstyrene-CMEs matched for sex and time point, & denotes significant differences between male and female mice matched for exposure and time point, and $ denotes significant differences between 1- and 7-day postexposure time points matched for exposure and sex ($p < .05$).

generate unique serum metabolite profiles. For example, phenol, 5-hydroxy-3-[[5-(4-nitrophenyl)furan-2-yl]methylideneamino]-1H-imidazol-2-one, and 6-[4-(carboxymethyl)phenoxy]-3,4,5-trihydroxyoxane-2-carboxylic acid were upregulated in both male and female mice exposed to styrene-CMEs and may represent styrene-CME-specific biomarkers. 5-Hydroxy-3-[[5-(4-nitrophenyl)furan-2-yl]methylideneamino]-1H-imidazol-2-one is a nitrobenzene and inhalation induces headache, nausea, fatigue dizziness, cyanosis, weakness in the arms and legs, and rare cases may be fatal (Public Health England, 2018). Previous studies have demonstrated exposure to VOCs such as vinyl chloride, benzene, carbon tetrachloride, and perchloroethylene are known to cause changes in lipid metabolites regulating inflammatory responses, oxidative stress, and insulin resistance (Guardiola *et al.*, 2016; Lang and Beier, 2018). The untargeted metabolite profiling data demonstrated males and females responded differently to exposures. For example, homovanillin was significantly elevated in females following exposure to styrene-CMEs. Previously, homovanillic acid, generated from homovanillin, was identified as a marker of metabolic stress (Marcelis *et al.*, 2006). Additionally, the profiling data demonstrated mice responded differently at 1- and 7-day postexposure time points. FAHFA 34:4; O and phosphatidic acid 24:0 were not found to remain significantly altered in female mice exposed to either emission at the 7-day time point suggesting some potential recovery at this time point in females. Our current study investigated a single exposure to CMEs and identified unique alterations in biomarker profiles that were resin-, sex-, and time-specific. There is a need for additional experiments to confirm and translate results to humans. Further, there is a need to establish circulating metabolite/lipid alterations that are dependent on distinct emission components to inform modifications to the composite manufacturing procedures.

Our previous *in vitro* assessment utilizing styrene CIPP emission condensates collected from steam curing worksites demonstrated alterations in cytotoxicity, the proteome, and inflammatory gene expression (Kobos *et al.*, 2019). In the present study, styrene-CME exposure caused an increase in inflammatory and oxidative stress markers (*Cxcl2*, *Il6*, *Ccl2*, *Tnfα*, *Vcam1*, *Cxcl1*, *Tgmt2*, *Hmox1*, and *Tgfβ1*) in lung tissue. A previous study reported 2 workers in factories manufacturing styrene-related products exhibited the development of acute respiratory symptoms associated with the impaired gas exchange as well as imaging and histopathologic findings consistent with bronchiolitis and pneumonia following exposure to gas-phase styrene (Meyer *et al.*, 2018). These findings from 2 workers demonstrate

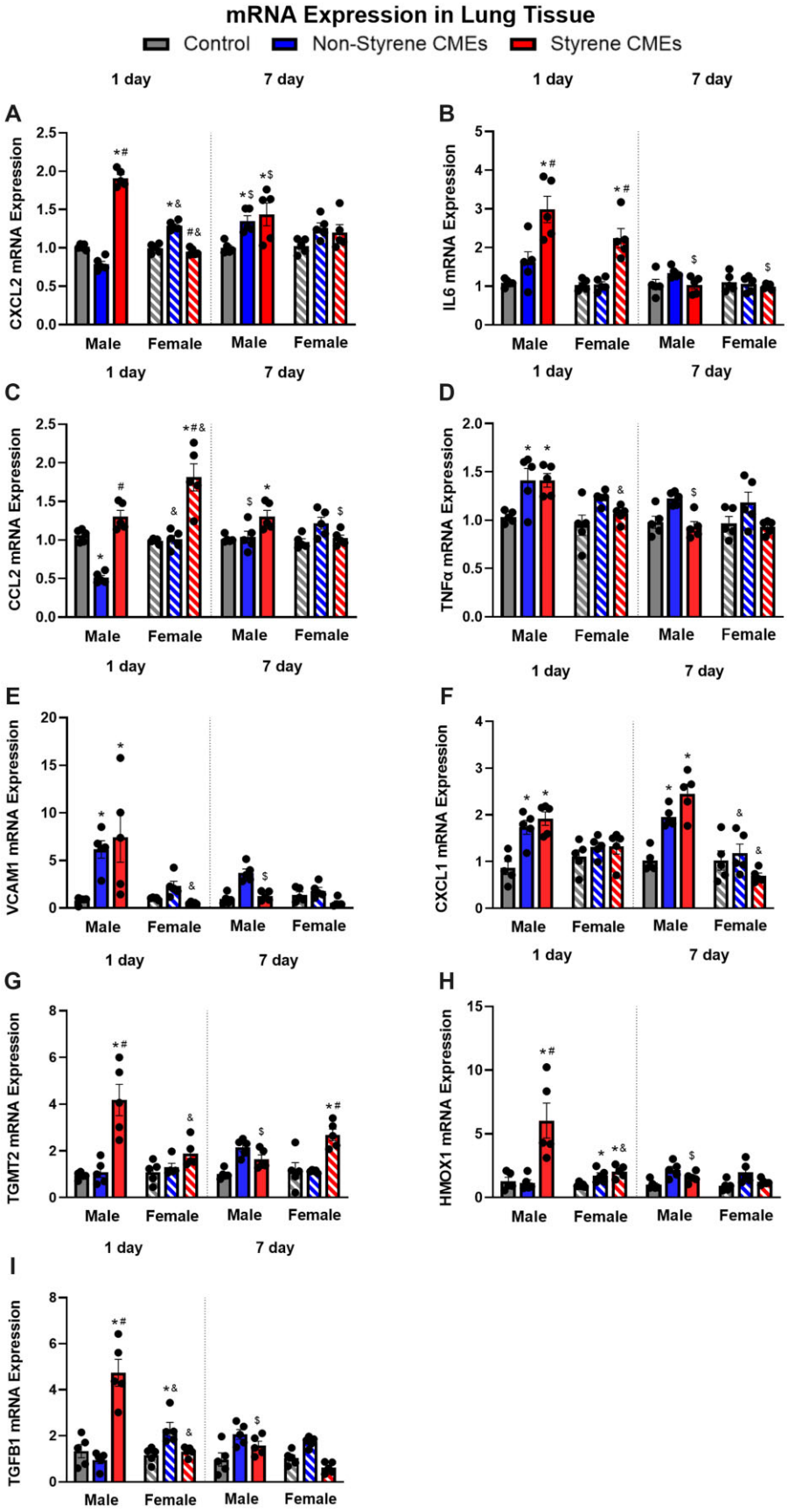

Figure 6. mRNA expression of *Cxcl2* (A), *Il6* (B), *Ccl2* (C), *Tnfα* (D), *Vcam1* (E), *Cxcl1* (F), *Tgmt2* (G), *Hmox1* (H), and *Tgfβ1* (I) in lung tissue after 1 day or 7 days following exposure to styrene-CMEs or nonstyrene-CMEs in male and female mice ($n = 5$/group). * denotes significant differences because of exposures compared with the control group matched for sex and time point, # denotes significant differences between styrene-CMEs and nonstyrene-CMEs matched for sex and time point, & denotes significant differences between male and female mice matched for exposure and time point, and $ denotes significant differences between 1- and 7-day postexposure time points matched for exposure and sex ($p < .05$).

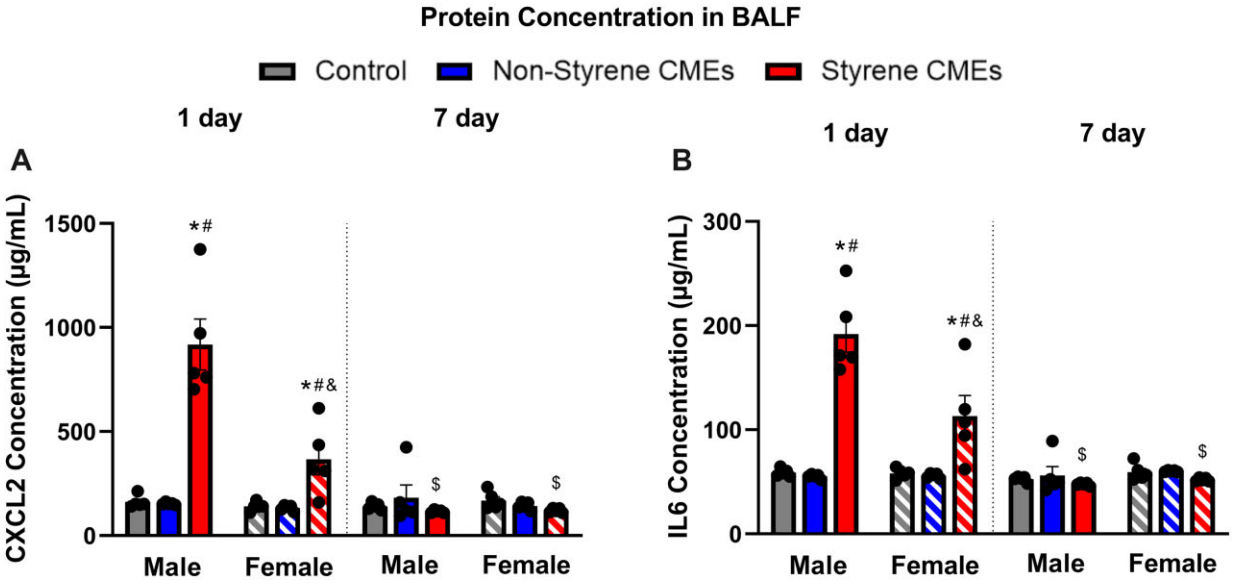

Figure 7. Bronchoalveolar lavage fluid protein concentrations of CXCL2 (A) and IL6 (B) in BALF 1 day or 7 days following styrene-CMEs or nonstyrene-CMEs in male and female mice ($n = 5$/group). * denotes significant differences because of exposures compared with the control group matched for sex and time point, # denotes significant differences between styrene-CMEs and nonstyrene-CMEs matched for sex and time point, & denotes significant differences between male and female mice matched for exposure and time point, and $ denotes significant differences between 1- and 7-day postexposure time points matched for exposure and sex ($p < .05$).

pulmonary inflammation and damage following styrene inhalation. Further, the 8-h time-weighted average was 29.3 ppm at the facility, which is comparable to the peak inhalation exposure concentration utilized in our study. Results from the present study also revealed altered pulmonary injury (increased total protein) and inflammation (lymphocyte influx and gene expression) following exposure to styrene-CMEs compared with the nonstyrene-CMEs. Influx of lymphocytes is involved in chronic inflammatory lesions (Koyasu and Moro, 2012). A previous study demonstrated an increased total nucleated cell count, with 28% lymphocytes in the BALF of a worker exposed to fiberglass resins (Meyer *et al.*, 2018). A reduction in BALF macrophages following exposure to CMEs was observed in our study. Decreased macrophage numbers in BALF may be related exposure-induced activation. Specifically, previous inhalation studies have demonstrated macrophages are activated following CME exposure inducing adhesion processes which may reduce our ability to collect them via the lavage procedure (Ma *et al.*, 2023; Miyata and van Eeden, 2011; Orecchioni *et al.*, 2019). Additionally, intercellular adhesion molecule-1 has been shown to be upregulated in lung injury and is an important adhesion molecule for lung epithelial cells and macrophages that may result in firm adhesion *in vivo* (Hamanaka, 2010). Our data demonstrate elevations in cytokines produced by macrophages suggestive of activation and enhanced adhesion within the lung that may reduce lavage collection of macrophages. Specifically, macrophages are associated with proinflammatory responses and produce cytokines such as *Il6* and *Tnfα*. The gene expression of both cytokines was found to be elevated following exposures to both emissions at 1-day postexposure suggesting increased macrophage activation. Additionally, lymphocyte recruitment can be facilitated by increases in IL6 (McLoughlin *et al.*, 2005). IL6 and CXCL2 presented robust changes in protein levels following exposure to styrene-CMEs, which may cause subsequent signaling through STAT3, NF-kB, and ERK1/2 (Fetoni *et al.*, 2021; Niaz *et al.*, 2017). These pathways have been studied and determined to be involved in inducing adverse effects of styrene exposure (Fetoni *et al.*, 2021; Niaz *et al.*, 2017; Xie *et al.*, 2020). It is noteworthy that gene expression data showed some recovery at 7-day postexposure, whereas expression of some genes such as *Ccl2* and *Cxcl1* remained significantly elevated in males but not females following exposure to styrene-CMEs. This suggests males and females may have differential recovery following exposure. Also, differential inflammatory responses and oxidative stress were determined 1- or 7-day postexposure to CMEs. Specifically, gene levels of *Il6*, *Vcam1*, *Tgfβ1*, and *Hmox1* did not show significant changes 7 days following CME exposures, revealing a trend toward recovery in these responses. However, markers including *Cxcl2* and *Cxcl1* were still enhanced compared with the levels in the control group, suggesting some elevations in markers of inflammation and oxidative stress persist 7 days after exposures. Lastly, there was consistency across endpoints evaluated supporting acute pulmonary responses after a single CME exposure. Specifically, lung tissue gene expression (performed in the unlavaged left lung) demonstrated alterations that were consistent with changes observed between groups in the cell counts and protein assessments performed in the BALF collected from the right lung lobes. Overall pulmonary results were also consistent with alterations observed in serum metabolites and lipids.

Several VOCs such as acetophenone, benzaldehyde, styrene oxide, cumene, α-methylstyrene, TMB, 1,3,5-TMB, and phenol were detected in a previous study while curing styrene-CMEs (Noh *et al.*, 2023). However, no other chemicals except for styrene were found emitted into the air during the production of the nonstyrene-CME (Noh *et al.*, 2023). A single sorbent tube was utilized during our current experiment, which may have resulted in sorbent bed saturation and interfered with the methods capacity to identify nonstyrene components of the CMEs. To understand CME toxicity responses, the detection of other VOCs, beyond styrene, in air is necessary as they may contribute to differential toxicity. VOCs are lipophilic and can cross the blood-brain barrier and cause neurological effects (Ajdari, 2016; Oppenheim *et al.*, 2013). Neurological effects of CMEs were observed in this study. Gene expression of *Vcam1* and *Tnfα* was elevated following

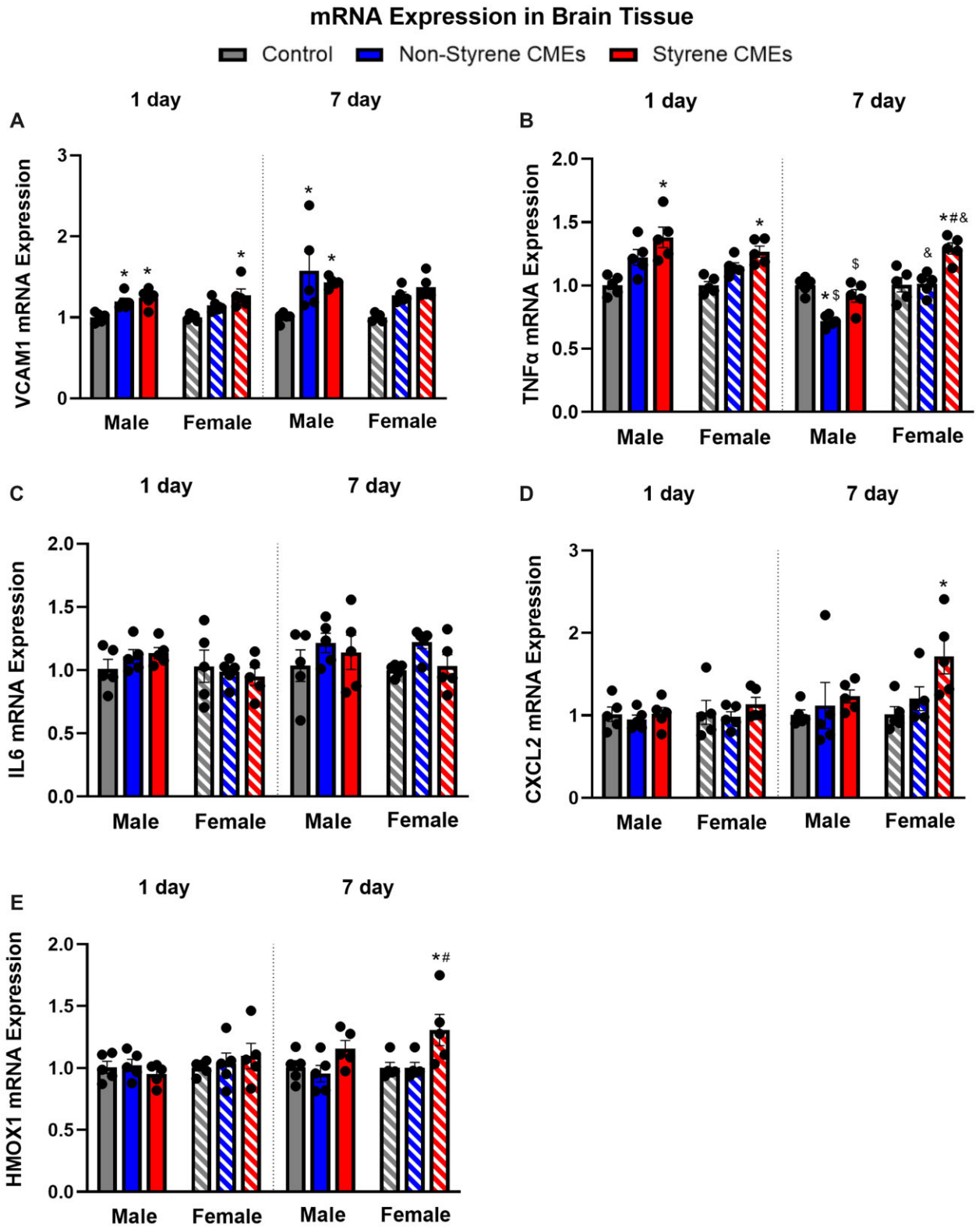

Figure 8. mRNA expression of *Cxcl2* (A), *Tnfα* (B), *Il6* (C), *Cxcl2* (D), and *Hmox1* in brain tissue 1 day or 7 days following exposure to styrene-CMEs or nonstyrene-CMEs in male and female mice ($n = 5$/group). * denotes significant differences because of exposures compared with the control group matched for sex and time point, # denotes significant differences between styrene-CMEs and nonstyrene-CMEs matched for sex and time point, & denotes significant differences between male and female mice matched for exposure and time point, and $ denotes significant differences between 1- and 7-day postexposure time points matched for exposure and sex ($p < .05$).

exposure to CMEs suggesting an inflammatory response. Styrene-induced neurotoxicity following both short- and long-term exposures has been reported in workers since the 1970s and by individuals exposed to CIPP emissions (Rosemond, 2010). Our study suggests the potential for acute neurological toxicity following exposure to CMEs generated from both resins.

At or near actual manufacturing sites producing CMEs, bystanders and workers may be exposed to higher levels of emissions compared with the concentrations utilized in this study, potentially exacerbating health effects. A limitation of the present study was that steam was not utilized for manufacture, and it is also one of the most utilized methods for curing. Uncured resin and nanoplastics have also been found to be discharged into the air by the steam-cured CIPP process, and were not characterized here (Morales *et al.*, 2022; Teimouri Sendesi *et al.*, 2017). The current study represents our initial evaluation of the toxicity associated with CME exposure through examination of fundamental inflammatory and oxidative stress markers. The information from this study supports the need for further evaluations to examine more endpoints. Specifically, histopathological examination of lung and brain should be considered in the future to better understand pulmonary and neurological toxicity after single or repeated exposures. These assessments will need to evaluate repeated and single exposures where histological examination will be vital to determine risks such as those that may occur in occupational settings (near or at worksites) and for bystanders (near the worksite and in contaminated buildings). Overall, acute pulmonary and neurological toxicities were determined 1 day after exposure to both CMEs in both sexes. Some alterations indicating inflammation and oxidative stress persist 7 days after exposures, however, do trend toward recovery. Additional studies are necessary to examine the risks associated with CME exposures for the public and workers and to identify other modifiable factors which may reduce exposure-related health risks.

Supplementary data

Supplementary data are available at *Toxicological Sciences* online.

Declaration of conflicting interests

The authors declare the following information which may be considered as potential competing interests: AJW and BEB are named in a patent application (PCT/US18/28173) filed April 18, 2018 by the Purdue Research Foundation. The patent application pertains to the technologies for capturing, identifying, analyzing, and addressing emissions that are potentially hazardous to the environment and humans. The invention was developed with support from National Science Foundation (CBET-1624183).

Acknowledgments

The authors would like to acknowledge the support from Dr Nadezhda N. Zyaykina for training and guidance related to the use of GC-MS to evaluate the CMEs generated. Additionally, the authors would like to acknowledge the Purdue Metabolite Profiling Facility for assistance with the targeted and untargeted metabolite analysis.

Funding

This work was funded by the National Institute of Environmental Health Sciences (NIEHS) R03/ES030783.01.

REFERENCES

Aalto-Korte, K., Pesonen, M., and Suuronen, K. (2015). Occupational allergic contact dermatitis caused by epoxy chemicals: Occupations, sensitizing products, and diagnosis. *Contact Derm.* **73**, 336–342. https://doi.org/10.1111/cod.12445

ACGIH. (2013). *2013 TLVs and BEIs*. ACGIH Signature Publications, Cincinnati, OH. 242 p.

Ajdari, E. B. (2016). Volatile organic compound (VOC) emission during cured-in-place-pipe (CIPP) sewer pipe rehabilitation. ProQuest Dissertations and Theses, 159. https://search.proquest.com/docview/1845871545?accountid=14449. Accessed March 27, 2023.

Berglind, I. A., Lind, M. L., and Lidén, C. (2012). Epoxy pipe relining-an emerging contact allergy risk for workers. *Contact Derm.* **67**, 59–65. https://doi.org/10.1111/j.1600-0536.2011.02028.x

Bruno, K. A., Mathews, J. E., Yang, A. L., Frisancho, J. A., Scott, A. J., Greyner, H. D., Molina, F. A., Greenaway, M. S., Cooper, G. M., Bucek, A., *et al.* (2019). BPA alters estrogen receptor expression in the heart after viral infection activating cardiac mast cells and T cells leading to perimyocarditis and fibrosis. *Front. Endocrinol.* **10**, 1–18. https://doi.org/10.3389/fendo.2019.00598

California Department of Public Health (CDPH). (2017). *Cured-In-Place-Pipe (CIPP) Additional Consideration for Municipalities*. California Department of Public Health, Sacramento, CA.

California Department of Public Health (CDPH). (2020). *Safety Alert Cured-In-Place Pipe (CIPP) Vapor Migration into Building*. California Department of Public Health, Sacramento, CA.

Chakrabarti, S. K. (2000). Altered regulation of dopaminergic activity and impairment in motor function in rats after subchronic exposure to styrene. *Pharmacol. Biochem. Behav.* **66**, 523–532. https://doi.org/10.1016/S0091-3057(00)00216-1

Cherry, N., and Gautrin, D. (1990). Neurotoxic effects of styrene: further evidence. *Br. J. Ind. Med.* **47**, 29–37. https://doi.org/10.1136/oem.47.1.29.

CIEL, EIP, FracTracker Alliance, GAIA, 5Gyres, & Breakfreefromplastic. (2019). Plastic & climate: The hidden costs of a plastic planet. *CIEL, Earthworks, GAIA, HBBF, IPEN, t.e.j.a.s., Upstream, & Breakfreefromplastic*. 1–108. https://www.ciel.org/wp-content/uploads/2019/05/Plastic-and-Climate-FINAL-2019.pdf. Accessed March 27, 2023.

Collins, J. J., Bodner, K. M., Bus, J. S., Collins, J. J., Bodner, K. M., and Bus, J. S. (2013). Linked references are available on JSTOR for this article: Cancer mortality of workers exposed to styrene in U.S. *Reinf. Plast. Comp. Ind.* **24**, 195–203. https://doi.org/10.1097/EDE.0b013e31828

Farcas, M. T., McKinney, W., Qi, C., Mandler, K. W., Battelli, L., Friend, S. A., Stefaniak, A. B., Jackson, M., Orandle, M., Winn, A., *et al.* (2020). Pulmonary and systemic toxicity in rats following inhalation exposure of 3-D printer emissions from acrylonitrile butadiene styrene (ABS) filament. *Inhal. Toxicol.* **32**, 403–418. https://doi.org/10.1080/08958378.2020.1834034

Fetoni, A. R., Paciello, F., Rolesi, R., Pisani, A., Moleti, A., Sisto, R., Troiani, D., Paludetti, G., and Grassi, C. (2021). Styrene targets sensory and neural cochlear function through the crossroad between oxidative stress and inflammation. *Free Radic. Biol. Med.* **163**, 31–42. https://doi.org/10.1016/j.freeradbiomed.2020.12.001

Fillenham, G., Lidén, C., and Anveden Berglind, I. (2012). Skin exposure to epoxy in the pipe relining trade-an observational study. *Contact Derm.* **67**, 66–72. https://doi.org/10.1111/j.1600-0536.2012.02065.x

Florida Department of Public Health (FDOH). (2020). *Cured-In-Place-Pipe [CIPP]*. Florida Department of Public Health, Marriottsville, MD. https://www.floridahealth.gov/environmental-health/

hazardous-waste-sites/_documents/final_fdoh_cipp.pdf. Accessed March 27, 2023.

Gowdy, K., Krantz, Q. T., Daniels, M., Linak, W. P., Jaspers, I., and Gilmour, M. I. (2008). Modulation of pulmonary inflammatory responses and antimicrobial defenses in mice exposed to diesel exhaust. *Toxicol. Appl. Pharmacol.* **229**, 310–319.

Guardiola, J. J., Beier, J. I., Falkner, K. C., Wheeler, B., McClain, C. J., and Cave, M. (2016). Occupational exposures at a polyvinyl chloride production facility are associated with significant changes to the plasma metabolome. *Toxicol. Appl. Pharmacol.* **313**, 47–56. https://doi.org/10.1016/j.taap.2016.10.001

Hahladakis, J. N., Velis, C. A., Weber, R., Iacovidou, E., and Purnell, P. (2018). An overview of chemical additives present in plastics: Migration, release, fate and environmental impact during their use, disposal and recycling. *J. Hazard. Mater.* **344**, 179–199. https://doi.org/10.1016/j.jhazmat.2017.10.014

Hamanaka, K., Jian, M.-Y., Townsley, M. I., King, J. A., Liedtke, W., Weber, D. S., Eyal, F. G., Clapp, M. M., and Parker, J. C. (2010). TRPV4 channels augment macrophage activation and ventilator-induced lung injury. *Am. J. Physiol. Lung Cell. Mol. Physiol.* **299**, L353–L362.

Hoecke, L. V., Job, E. R., Saelens, X., and Roose, K. (2017). Bronchoalveolar lavage of murine lungs to analyze inflammatory cell infiltration. *J. Vis. Exp.* **123**, e55398.

IARC. (2002). International Agency for Research on Cancer IARC Monographs on the Evaluation of Carcinogenic Risks To Humans. Volume 82. http://monographs.iarc.fr/ENG/Monographs/vol83/mono83-1.pdf. Accessed March 27, 2023.

Jaakkola, J. J., and Knight, T. L. (2008). The role of exposure to phthalates from polyvinyl chloride products in the development of asthma and allergies: A systematic review and meta-analysis. *Environ. Health Perspect.* **116**, 845–853.

Kobos, L., Teimouri Sendesi, S. M., Whelton, A. J., Boor, B. E., Howarter, J. A., and Shannahan, J. (2019). In vitro toxicity assessment of emitted materials collected during the manufacture of water pipe plastic linings. *Inhal. Toxicol.* **31**, 131–146. https://doi.org/10.1080/08958378.2019.1621966

Kogevinas, M., Ferro, G., Andersen, A., Bellander, T., Coggon, D., Gennaro, V., Hutchings, S., Kolstad, H., Lynge, E., Partanen, T., *et al.* (1994). Cancer mortality in a historical cohort study of workers exposed to styrene. *Scand. J. Work Environ. Health* **20**, 251–261.

Kohn, J., Minotti, S., and Durham, H. (1995). Assessment of the neurotoxicity of styrene, styrene oxide, and styrene glycol in primary cultures of motor and sensory neurons. *Toxicol. Lett.* **75**, 29–37. https://doi.org/10.1016/0378-4274(94)03153-X

Komura, K., Yanaba, K., Horikawa, M., Ogawa, F., Fujimoto, M., Tedder, T. F., and Sato, S. (2008). CD19 regulates the development of bleomycin-induced pulmonary fibrosis in a mouse model. *Arthritis Rheum.* **58**, 3574–3584.

Koyasu, S., and Moro, K. (2012). Role of innate lymphocytes in infection and inflammation. *Front. Immunol.* **3**, 1–13. https://doi.org/10.3389/fimmu.2012.00101

Lang, A. L., and Beier, J. I. (2018). Interaction of volatile organic compounds and underlying liver disease: a new paradigm for risk. *Biol. Chem.* **399**, 1237–1248.

Lebouf, R. F., and Burns, D. A. (2019). *Evaluation of Exposures to Styrene during Ultraviolet Cured-in-place Pipe Installation.* National Institute for Occupational Safety and Health. https://www.cdc.gov/niosh/hhe/reports/pdfs/2018-0009-3334_revised032019.pdf. Accessed March 27, 2023.

Lenth, R., Singmann, H., Love, J., Buerkner, P., and Herve, M., (2022). Package 'Emmeans' R topics documented. *Am. Stat.* **34**, 216–221. https://cran.microsoft.com/snapshot/2018-01-13/web/packages/emmeans/emmeans.pdf. Accessed March 27, 2023.

Lim, H. K., Choi, Y. A., Park, W., Lee, T., Ryu, S. H., Kim, S. Y., Kim, J. R., Kim, J. H., and Baek, S. H. (2003). Phosphatidic acid regulates systemic inflammatory responses by modulating the Akt-mammalian target of rapamycin-p70 S6 kinase 1 pathway. *J. Biol. Chem.* **278**, 45117–45127. https://doi.org/10.1074/jbc.M303789200

Lithner, D., Larsson, A., and Dave, G. (2011). Environmental and health hazard ranking and assessment of plastic polymers based on chemical composition. *Sci. Total Environ.* **409**, 3309–3324. https://doi.org/10.1016/j.scitotenv.2011.04.038

Lundberg, R., Bahl, M. I., Licht, T. R., Toft, M. F., and Hansen, A. K. (2017). Microbiota composition of simultaneously colonized mice housed under either a gnotobiotic isolator or individually ventilated cage regime. *Sci. Rep.* **7**, 42245–42211. https://doi.org/10.1038/srep42245

Ma, J., Chen, T., Mandelin, J., Ceponis, A., Miller, N. E., Hukkanen, M., Ma, G. F., and Konttinen, Y. T. (2003). Regulation of macrophage activation. *Cell. Mol. Life Sci.* **60**, 2334–2346.

Marcelis, M., Suckling, J., Hofman, P., Woodruff, P., Bullmore, E., and van Os, J. (2006). Evidence that brain tissue volumes are associated with HVA reactivity to metabolic stress in schizophrenia. *Schizophr. Res.* **86**, 45–53. https://doi.org/10.1016/j.schres.2006.05.001

Matthews, E., Matthews, J., Alam, S., and Eklund, S. (2020). NASSCO CIPP emissions phase 2: Evaluation of air emissions from polyester resin CIPP with steam. Trenchless Technology Center Research Report, 693.

McLoughlin, R. M., Jenkins, B. J., Grail, D., Williams, A. S., Fielding, C. A., Parker, C. R., Ernst, M., Topley, N., and Jones, S. A. (2005). IL-6 trans-signaling via STAT3 directs T cell infiltration in acute inflammation. *Proc. Natl. Acad. Sci. USA* **102**, 9589–9594. https://doi.org/10.1073/pnas.0501794102

Meeker, J. D., Sathyanarayana, S., and Swan, S. H. (2009). Phthalates and other additives in plastics: Human exposure and associated health outcomes. *Philos. Trans. R. Soc. B Biol. Sci.* **364**, 2097–2113. https://doi.org/10.1098/rstb.2008.0268

Meyer, K. C., Sharma, B., Kaufmann, B., Kupper, A., and Hodgson, M. (2018). Lung disease associated with occupational styrene exposure. *Am. J. Ind. Med.* **61**, 773–779. https://doi.org/10.1002/ajim.22867

Miyata, R., and van Eeden, S. F. (2011). The innate and adaptive immune response induced by alveolar macrophages exposed to ambient particulate matter. *Toxicol. Appl. Pharmacol.* **257**, 209–226.

Moore, C. J. (2008). Synthetic polymers in the marine environment: A rapidly increasing, long-term threat. *Environ. Res.* **108**, 131–139. https://doi.org/10.1016/j.envres.2008.07.025

Morales, A. C., Tomlin, J. M., West, C. P., Rivera-Adorno, F. A., Peterson, B. N., Sharpe, S. A. L., Noh, Y., Sendesi, S. M. T., Boor, B. E., Howarter, J. A., *et al.* (2022). Atmospheric emission of nanoplastics from sewer pipe repairs. *Nat. Nanotechnol.* **17**, 1171–1177. https://doi.org/10.1038/s41565-022-01219-9

Morgan, D. L., Mahler, J. F., Dill, J. A., Price Jr, H. C., O'Connor, R. W., and Adkins Jr, B. (1993a). Styrene inhalation toxicity studies in mice: II. Sex differences in susceptibility of B6C3F1 mice. *Fundam. Appl. Toxicol.* **21**, 317–325.

Morgan, D. L., Mahler, J. F., O'Connor, R. W., Price, H. C., and Adkins, B. (1993b). Styrene inhalation toxicity studies in mice: I. Hepatotoxicity in b6c3f1 mice. *Toxicol. Sci.* **20**, 325–335. https://doi.org/10.1093/toxsci/20.3.325

Niaz, K., Hassan, F. I., Mabqool, F., Khan, F., Momtaz, S., Baeeri, M., Navaei-Nigjeh, M., Rahimifard, M., and Abdollahi, M. (2017). Effect of styrene exposure on plasma parameters, molecular mechanisms and gene expression in rat model islet cells. *Environ. Toxicol. Pharmacol.* **54**, 62–73. https://doi.org/10.1016/j.etap.2017.06.020

NIEHS. (2021). Report on Carcinogens, Fifteenth Edition: Formaldehyde. National Toxicology Program, Department of Health and Human Services. https://ntp.niehs.nih.gov/ntp/roc/content/profiles/formaldehyde.pdf. Accessed March 27, 2023.

Noh, Y., Xia, L., Zyaykina, N. N., Boor, B. E., Shannahan, J. H., and Whelton, A. J. (2023). Regulatory significance of plastic manufacturing air pollution discharged into terrestrial environments and real-time sensing challenges. *Environ. Sci. Technol. Lett.* **10**, 152–158.

Noh, Y., Boor, B. E., Shannahan, J. H., Troy, C. D., Jafvert, C. T., and Whelton, A. J. (2022b). Emergency responder and public health considerations for plastic sewer lining chemical waste exposures in indoor environments. *J. Hazard. Mater.* **422**, 126832. https://doi.org/10.1016/j.jhazmat.2021.126832

Noh, Y., Odimayomi, T., Teimouri Sendesi, S. M., Youngblood, J. P., and Whelton, A. J. (2022c). Environmental and human health risks of plastic composites can be reduced by optimizing manufacturing conditions. *J. Clean. Prod.* **356**, 131803. https://doi.org/10.1016/j.jclepro.2022.131803

Noh, Y., Shannahan, J. H., Hoover, A. G., Pennell, K. G., Weir, M. H., and Whelton, A. J. (2022a). Bystander chemical exposures and injuries associated with nearby plastic sewer pipe manufacture: public health practice and lessons. *J. Environ. Health* **85**, 22–31.

Nuruddin, M., Mendis, G. P., Ra, K., Sendesi, S. M. T., Futch, T., Goodsell, J., Whelton, A. J., Youngblood, J. P., and Howarter, J. A. (2019). Evaluation of the physical, chemical, mechanical, and thermal properties of steam-cured PET/polyester cured-in-place pipe. *J. Compos. Mater.* **53**, 2687–2699. https://doi.org/10.1177/0021998319839132

Oppenheim, H. A., Lucero, J. A., Guyot, A. C., Herbert, L. M., McDonald, J. D., Mabondzo, A., and Lund, A. K. (2013). Exposure to vehicle emissions results in altered blood brain barrier permeability and expression of matrix metalloproteinases and tight junction proteins in mice. *Part. Fibre Toxicol.* **10**, 1–14. https://doi.org/10.1186/1743-8977-10-62

Orecchioni, M., Ghosheh, Y., Pramod, A. B., and Ley, K. (2019). Macrophage polarization: different gene signatures in M1(Lps+) vs. classically and M2(LPS-) vs. alternatively activated macrophages. *Front. Immunol.* **10**, 1084–1014. https://doi.org/10.3389/fimmu.2019.01084

Patel, A. (2004). Serum triglycerides as a risk factor for cardiovascular diseases in the Asia-Pacific region. *Circulation* **110**, 2678–2686. https://doi.org/10.1161/01.CIR.0000145615.33955.83

Persoons, R., Richard, J., Herve, C., Montlevier, S., Marques, M., and Maitre, A. (2018). Biomonitoring of styrene occupational exposures: biomarkers and determinants. *Toxicol. Lett.* **298**, 99–105. https://doi.org/10.1016/j.toxlet.2018.06.1211

Priyanka, M., and Dey, S. (2018). Ruminal impaction due to plastic materials—an increasing threat to ruminants and its impact on human health in developing countries. *Vet. World* **11**, 1307–1315. https://doi.org/10.14202/vetworld.2018.1307-1315

Public Health England. (2018). *Nitrobenzene Toxicological Overview Key Points*. https://assets.publishing.service.gov.uk/government/uploads/system/uploads/attachment_data/file/760898/Nitrobenzene_toxicological_overview.pdf. Accessed March 27, 2023.

R Core Team. (2015). *R: A Language and Environment for Statistical Computing*. R Foundation for Statistical Computing, Vienna, Austria.

Ra, K., Teimouri Sendesi, S. M., Nuruddin, M., Zyaykina, N. N., Conkling, E. N., Boor, B. E., Jafvert, C. T., Howarter, J. A., Youngblood, J. P., and Whelton, A. J. (2019). Considerations for emission monitoring and liner analysis of thermally manufactured sewer cured-in-place-pipes (CIPP). *J. Hazard. Mater.* **371**, 540–549. https://doi.org/10.1016/j.jhazmat.2019.02.097

Ramadan, M., Cooper, B., and Posnack, N. G. (2020). Bisphenols and phthalates: plastic chemical exposures can contribute to adverse cardiovascular health outcomes. *Birth Defects Res.* **112**, 1362–1385. https://doi.org/10.1002/bdr2.1752

Rosemond, Z. A. (2010). *Toxicological Profile for Styrene*. Agency for Toxic Substances and Disease Registry. https://www.atsdr.cdc.gov/toxprofiles/tp53.pdf. Accessed March 27, 2023.

Russell, K., Yaeger, M. J., Hodge, M. X., Kilburg-Basnyat, B., Reece, S. W., Birukova, A., Guttenberg, M. A., Novak, C., Chung, S., Ehrmann, B. M., *et al.* (2023). Scavenger receptor BI attenuates oxidized phospholipid-induced pulmonary inflammation. *Toxicol. Appl. Pharmacol.* **462**, 116381.

Sati, P. C., Khaliq, F., Vaney, N., Ahmed, T., Tripathi, A. K., and Banerjee, B. D. (2011). Pulmonary function and oxidative stress in workers exposed to styrene in plastic factory: Occupational hazards in styrene-exposed plastic factory workers. *Hum. Exp. Toxicol.* **30**, 1743–1750. https://doi.org/10.1177/0960327111401436

Stratview Research. (2022). Markets reports. *Cured-in-Place Pipe Market Size, Share, Trend, Forecast, Competitive Analysis, and Growth Opportunity: 2022–2027*. https://www.stratviewresearch.com/287/Cured-in-Place-Pipe-CIPP-Market.html. Accessed March 27, 2023.

Sumner, S. J., and Fennell, T. R. (1994). Review of the metabolic fate of styrene. *Crit. Rev. Toxicol.* **24**, S1. https://doi.org/10.3109/10408449409020138

Tabor, M. L., Newman, D., and Whelton, A. J. (2014). Stormwater chemical contamination caused by cured-in-place pipe (CIPP) infrastructure rehabilitation activities. *Environ. Sci. Technol.* **48**, 10938–10947. https://doi.org/10.1021/es5018637

Teimouri Sendesi, S. M., Noh, Y., Nuruddin, M., Boor, B. E., Howarter, J. A., Youngblood, J. P., Jafvert, C. T., and Whelton, A. J. (2020). An emerging mobile air pollution source: outdoor plastic liner manufacturing sites discharge VOCs into urban and rural areas. *Environ. Sci. Process. Impacts* **22**, 1828–1841. https://doi.org/10.1039/d0em00190b

Teimouri Sendesi, S. M., Ra, K., Conkling, E. N., Boor, B. E., Nuruddin, M., Howarter, J. A., Youngblood, J. P., Kobos, L. M., Shannahan, J. H., Jafvert, C. T., *et al.* (2017). Worksite chemical air emissions and worker exposure during sanitary sewer and stormwater pipe rehabilitation using cured-in-place-pipe (CIPP). *Environ. Sci. Technol. Lett.* **4**, 325–333. https://doi.org/10.1021/acs.estlett.7b00237

Thompson, R. C., Moore, C. J., Saal, F. S. V., and Swan, S. H. (2009). Plastics, the environment and human health: Current consensus and future trends. *Philos. Trans. R. Soc. B Biol. Sci.* **364**, 2153–2166. https://doi.org/10.1098/rstb.2009.0053

Tighe, R. M., Birukova, A., Yaeger, M. J., Reece, S. W., and Gowdy, K. M. (2018). Euthanasia-and lavage-mediated effects on bronchoalveolar measures of lung injury and inflammation. *Am. J. Respir. Cell Mol. Biol.* **59**, 257–266.

Venables, W. N., and Ripley, B. D. (1997). *Tree-Based Methods*. Modern Applied Statistics with S-PLUS. https://doi.org/10.1007/978-1-4757-2719-7_14

Welty, F. K. (2013). How do elevated triglycerides and low HDL-cholesterol affect inflammation and atherothrombosis? *Curr. Cardiol. Rep.* **15**, 400. https://doi.org/10.1007/s11886-013-0400-4

Wood, P. L. (2020). Fatty acyl esters of hydroxy fatty acid (FAHFA) lipid review families. *Metabolites* **10**, 1–8. https://doi.org/10.3390/metabo10120512

Xie, X., Deng, T., Duan, J., Xie, J., Yuan, J., and Chen, M. (2020). Exposure to polystyrene microplastics causes reproductive toxicity through oxidative stress and activation of the p38 MAPK signaling pathway. *Ecotoxicol. Environ. Saf.* **190**, 110133. https://doi.org/10.1016/j.ecoenv.2019.110133

Yagielski, A. (2016). *The Influence of the Estrous Cycle on Acute Seizure Activity*. Syracuse University Honors Program Capstone Projects. 923. https://core.ac.uk/download/pdf/215706875.pdf. Accessed March 27, 2023.